#### الجمهورية الجزائرية الديمقراطية الشعبية

République Algérienne Démocratique et Populaire

وزارة التعليم العالي و البحث العلمي

Ministère de l'Enseignement Supérieur et de la Recherche Scientifique

#### Ecole Nationale Polytechnique

Department of Civil Engineering



المدرسة الوطنية المتعددة التقنيات Ecole Nationale Polytechnique

End-of-study project dissertation for obtaining the State Engineer's degree in Civil Engineering

Investigation of the effects of surface gravity waves on the distribution of hydrodynamic pressures by the finite element method : case of a vertical rigid dam

Presented by: Hadjer Dellil

Under the direction of Dr. Abdelmadjid TADJADIT MCB

Presented and defended publicly on (14/10/2025)

#### Composition of the jury:

President: Prof. Nouredine Bourahla

Examiner: Prof. Abdelkrim BOURZAM

Guest: Ms. Racha ZEGHMAR

ENP 2025

#### الجمهورية الجزائرية الديمقراطية الشعبية

République Algérienne Démocratique et Populaire

وزارة التعليم العالي و البحث العلمي

Ministère de l'Enseignement Supérieur et de la Recherche Scientifique

#### Ecole Nationale Polytechnique

Department of Civil Engineering



المدرسة الوطنية المتعددة التقنيات Ecole Nationale Polytechnique

End-of-study project dissertation for obtaining the State Engineer's degree in Civil Engineering

Investigation of the effects of surface gravity waves on the distribution of hydrodynamic pressures by the finite element method : case of a vertical rigid dam

Presented by: Hadjer Dellil

Under the direction of Dr. Abdelmadjid TADJADIT MCB

Presented and defended publicly on (14/10/2025)

#### Composition of the jury:

President: Prof. Nouredine Bourahla

Examiner: Prof. Abdelkrim BOURZAM

Guest: Ms. Racha ZEGHMAR

ENP 2025

#### الجمهورية الجزائرية الديمقراطية الشعبية

République Algérienne Démocratique et Populaire

وزارة التعليم العالي و البحث العلمي

Ministère de l'Enseignement Supérieur et de la Recherche Scientifique

#### Ecole Nationale Polytechnique

Département de Génie Civil



Mémoire de Projet de fin d'Etudes pour l'obtention du Diplôme d'Ingénieur d'Etat en Génie Civil

Étude des effets des ondes de gravité de surface sur la distribution des pressions hydrodynamiques par la méthode des éléments finis : cas d'un barrage rigide vertical

Présenté par : Hadjer Dellil

Sous la Direction de Dr. Abdelmadjid TADJADIT MCB

Présentée et soutenue publiquement le (14/10/2025)

#### Composition du jury:

Président : Prof. Nouredine Bourahla

Examinateur: Prof. Abdelkrim BOURZAM

Invité: Ms. Racha ZEGHMAR

ENP 2025

تتناول هذه الدراسة تأثير الموجات الجاذبية السطحية على الضغوط الهيدروديناميكية المطبقة على سد رأسي وطيد أثناء الحركات الأرضية الأفقية الاهتزازية. باستخدام طريقة العناصر المحدودة لتصميم خوارزمي للموائع القابلة للانضغاط وغير القابلة للانضغاط، تُقاس الاستجابات الهيدروديناميكية بشكل كمي. ومن خلال مراعاة تأثيرات الموجات السطحية عبر نموذج سطح حر خطي، يضمن التحليل اتساق هذه التأثيرات. يُعتبر سد الجاذبية نموذجًا لفهم كيفية ظهور تأثيرات الموجات المختلفة تحت ظروف متنوعة. بناءً على هذه النتائج، يُظهر التحليل أن للموجات السطحية التأثير الأكبر عند الترددات المنخفضة. عند هذه المستويات، يحدث انخفاض كبير في ضغوط القاعدة. مع ازدياد تردد الإثارة، يضعف تأثيرها وتصبح قابلية الانضغاط هي المسيطرة على الاستجابة، خاصةً أثناء الزلزال. يتوافق هذا السلوك مع الاتجاهات المذكورة في الدراسات المتخصصة ويُبرز ضرورة التمييز بين تأثيرات الموجات السطحية وتأثيرات الانضغاط عند تقييم سلامة السد.

الكلمات الاساسية: الموجات الجاذبية السطحية، الضغوط الهيدروديناميكية، السد وطيد، طريقة العناصر المحدودة، سد الفودة، الاستجابات الزلزالية.

#### Résumé

Cette étude analyse l'influence des ondes de gravité de surface sur les pressions hydrodynamiques exercées sur un barrage vertical rigide soumis à des mouvements horizontaux du sol. En recourant à la méthode des éléments finis pour modéliser des fluides incompressibles et compressibles, les réponses hydrodynamiques sont quantifiées. La prise en compte des effets des ondes de surface, via une condition de surface libre linéarisée, permet de garantir une meilleure précision dans l'évaluation des pressions hydrodynamiques. Le barrage-poids d'El Fodda constitue l'étude de cas; les résultats sont évalués dans les domaines temporel et fréquentiel afin de mettre en évidence les impacts critiques, en comparant des situations avec et sans effets des ondes de surface. Ces résultats fournissent une base solide pour interpréter la manifestation des différents effets d'ondes dans diverses conditions.

Sur la base de ces résultats, l'analyse montre que les ondes de surface exercent une influence maximale aux basses fréquences. À ces niveaux, on observe une réduction substantielle des pressions de base. À mesure que la fréquence d'excitation augmente, leur effet s'atténue, et la compressibilité devient le facteur prédominant dans la réponse, notamment lors d'événements sismiques. Ce comportement est conforme aux tendances rapportées dans la littérature spécialisée. Il souligne l'importance de distinguer les effets des ondes de surface de ceux de la compression lors de l'évaluation de la sécurité des barrages.

Mots clés : Ondes de gravité de surface, Pressions hydrodynamiques, Barrage rigide, Méthode des éléments finis, Barrage d'El Fodda, Réponses sismiques.

#### **Abstract**

This study examines the influence of surface gravity waves on the hydrodynamic pressures exerted on a rigid vertical dam during horizontal ground motions. Using the Finite Element Method for both incompressible and compressible fluid models, hydrodynamic responses are quantified. By accounting for surface-wave effects through a linearized free-surface condition, the analysis ensures their consistent influence. The El Fodda gravity dam serves as a case study, with outcomes assessed in both the time and frequency domains to highlight critical impacts, comparing situations with and without surface wave effects. These findings provide a foundation for interpreting how different wave effects manifest under various conditions.

Building on these results, the analysis shows that surface waves have the most influence at low frequencies. At these levels, there is a substantial reduction in base pressures. As excitation frequency increases, their effect weakens, and compressibility governs the response, especially during seismic events. This behavior matches trends reported in the specialized literature. It highlights the need to distinguish surface-waves and compressional effects when assessing dam safety.

**Keywords :** Surface gravity waves , Hydrodynamic pressures ,Rigid dam, Finite element method,El Fodda Dam ,Seismic responses.

#### Acknowledgments

At the conclusion of this modest work, I would like to express my sincere gratitude to my supervisor, Mr. Abdelmadjid Tadjadit, for his invaluable guidance, patience, and continuous encouragement throughout this project. His insightful advice and unwavering support have been instrumental in the successful completion of this dissertation.

I am sincerely thankful for the time and effort he dedicated to directing my work and for giving me the opportunity to learn and grow under his supervision.

Finally, I would also like to extend my appreciation to all the professors who contributed to my academic formation during my years of study at the Ecole Nationale Polytechnique.

Hadjer Dellil,

### **Dedications**

TO my research supervisor, for his constant support and valuable advice.

my beloved family, a source of endless strength and motivation.

TO my brother, for his presence and encouragement throughout this journey.

TO all those dear to me, to all of you.

Thank You.

- Hadjer Dellil,

## Table of Contents

T	ie	+	Λf	٦.	$\Gamma_{\mathbf{a}}$	hl	les
ь.	115				1	. , ,	

List of Figures

#### List of Symbols

$\mathbf{G}$	ENE	RAL I	NTROD	UCTION	14
	0.1	Motiva	ation		15
	0.2	Object	tives of th	e study	16
	0.3	Struct	ure of the	e dissertation	16
1	LIT	ERAT	URE RI	EVIEW	19
	1.1	Introd	uction		19
	1.2	Histor	ical conte	xt and major seismic accidents	19
	1.3	Classi	cal analyt	ical and semi-analytical approaches	19
		1.3.1	Early pi	oneers and their fundamental assumptions	20
			1.3.1.1	Westergaard's simplified model (1933)	20
			1.3.1.2	Zangar electrical analogy method (1952)	21
			1.3.1.3	von Kármán and Housner (1957)	21
			1.3.1.4	Kotsubo (1960)	21
			1.3.1.5	Anil K. Chopra (1966): hydrodynamic pressures on dams during earthquakes	22
			1.3.1.6	Nath (1969)	23
		1.3.2	Limitati	ons of classical approaches	23
		1.3.3	Develop	ment of numerical methods	24
	1.4	Integr	ation of s	urface wave effects in dam–reservoir analysis	25
		1.4.1	Bustama	ante et al. (1963): free-surface and compressibility effects	25

			1.4.1.0.1 Key findings	25
			1.4.1.0.2 Implications	26
		1.4.2	Chwang (1981, 1985) : Surface waves, compressibility, and flexibility	26
		1.4.3	Eatock Taylor (1981) : mode superposition and surface wave criteria	26
		1.4.4	Wu and Yu (1989) : Trefftz method and wave–Dam interaction $\ \ldots \ \ldots$	28
		1.4.5	Tsai and Wei (1991)	28
		1.4.6	Martin (1992): wavemaker analogy and surface wave criteria	28
		1.4.7	Maity and Bhattacharya (1999, 2003) : boundary conditions for FEM with surface waves	29
		1.4.8	Attarnejad and Zahedi (2004) : time-domain exact solution with surface waves	29
		1.4.9	Avilés and Suárez (2010) : surface waves in compressible and viscous fluids	30
		1.4.10	Gogoi and Maity (2006–2010) : truncation boundaries and frequency-domain approaches	30
		1.4.11	Pani and Bhattacharyya (2008): FEM with free-surface and truncated boundaries	31
		1.4.12	Chen and Yuan (2011); Abdollahi and Attarnejad (2012) : quantifying surface wave effects	31
		1.4.13	da Silva and Pedroso (2019)	31
	1.5	conclus	sion	32
<b>2</b>	MA	THEM	ATICAL MODEL AND GOVERNING EQUATIONS	35
	2.1		uction	
	2.2		ng assumptions and geometry	
		2.2.1	Geometry and computational domain	
	2.3	Theore	etical formulation	
		2.3.1	Governing equations for fluid	36
		2.3.2	Boundary conditions	37
	2.4	Conclu	sion	39
3	Nur	nerical	Analysis and Comparative Results	42
	3.1	Introd	uction	42
	3.2	Numer	ical model setup	42
	3.3	Baselir	ne case: without surface waves	44

	3.3.1	Incompressible fluid–without surface waves	45
		3.3.1.1 Determination of an appropriate reservoir length	45
		3.3.1.2 Determination of the optimal mesh	46
		3.3.1.3 Results for an optimal mesh	48
	3.3.2	Compressible fluid–without surface waves	48
		3.3.2.1 Case of a harmonic excitation	48
		3.3.2.2 Seismic excitation	48
3.4	Exten	ded case : with surface waves	50
	3.4.1	Incompressible fluid–with surface waves	52
		3.4.1.1 The wave-effect parameter	52
		3.4.1.2 Analysis of hydrodynamic pressure contours	53
		3.4.1.3 Analysis of the velocity vector field	53
		3.4.1.4 Hydrodynamic pressure profiles for harmonic Excitation	55
	3.4.2	Compressible fluid–with surface waves	59
		3.4.2.0.1 Compressibility parameter	59
3.5	Comp	arison with classical studies	61
	3.5.1	Nath (1969)	61
	3.5.2	Bustamante et al. (1963)	61
	3.5.3	Eatock Taylor (1981)	62
3.6	Conclu	usion	62
Genera	al Cond	clusion	64
Bibliog	graphie		66
Appen	dices		70
Annex	e - Ex	tension of the Work through Analytical Formulations	<b>7</b> 1
.1	Introd	luction	71
.2	Formu	ılation	71
.3	Result	SS	72
.4	Discus	ssion	73
.5	Conclu	usions	73

## List of Tables

3.1	Convergence of $C_{p_{\max}}$ in a function of reservoir length	46
3.2	Influence of the number of mesh nodes on the upstream face of the dam on the hydrodynamic pressure coefficient $C_p$	46
3.3	Comparison of maximum pressure coefficients with and without surface-wave effects in slow and fast regimes, obtained using the Triftz method	53
3.4	Maximum pressure coefficient $C_p^{\max}$ for a vertical dam under different values of the surface-wave parameter, assuming an incompressible, inviscid fluid	56
3.5	Computed values of the compressibility parameter $B$ for different values of $\sigma$	59
3.6	Peak hydrodynamic pressures under El Centro excitation for both case with and without surface waves	59

## List of Figures

2.1	Geometry of the dam-reservoir system	36
3.1	The Resolution algorithm by MATLAB	43
3.2	3D schematic of the dam—reservoir system with boundary conditions and interface representation	44
3.3	The dam–reservoir system	45
3.4	Comparison of hydrodynamic pressures for different lengths (L) $\ \ldots \ \ldots$	45
3.5	Dam reservoir	46
3.6	Finite element mesh showing refined elements near the dam-reservoir interface (H = 100 m, L = 300 m)	47
3.7	Contours of hydrodynamic isopressures	48
3.8	Response to harmonic excitations $f = 1, 3.6, 10 \mathrm{Hz}$	49
3.9	The seismic acceleration of El Centro, 1940	49
3.10	The response to a seismic excitation (EL CENTRO)	50
3.11	Fourier transform of the accelerogram	50
3.12	Variation of hydrodynamic pressures as a function of excitation frequency at the base of a vertical rigid dam	50
3.13	The resolution algorithm by MATLAB	51
3.14	The dam–reservoir system with a surface wave above the fixed free surface $\dots$	52
3.15	Evolution of hydrodynamic pressure contours with the surface-wave parameter $\sigma$	54
3.16	Frequency-dependent surface wave effects on velocity field in dam reservoir	55
3.17	Variation of the pressure coefficient with depth for different values of the surfacewave parameter	57
3.18	Hydrodynamic pressure response to surface waves for different values of the surface-wave parameter $\sigma$ assuming an incompressible, inviscid fluid	58
3.19	Seismic response of hydrodynamic pressures including compressibility and surfacewave effects	60

20	Methodological framework comparing FEM approach (vertical dams) and Trefftz	
	method (sloped dams)	72

## List of Symbols

#### Latin Symbols

H	Reservoir height [m]
L	Reservoir length [m]
p(x, y, t)	Hydrodynamic pressure in the time domain [Pa]
$p(x, y, \omega)$	Hydrodynamic pressure in the frequency domain [Pa]
$\ddot{u}_g$	Horizontal ground acceleration $[m/sec^2]$
$\ddot{u}_n$	Normal component of horizontal ground acceleration [m/sec <sup>2</sup> ]
g	Gravitational acceleration [m/sec <sup>2</sup> ]
C	Compression wave velocity $[m/sec^2]$
$C_p$	Hydrodynamic pressure coefficient
t	Time [sec]
f	Excitation frequency [Hz]
T	Excitation period [sec]
$F_r$	The Froude number

#### Greek Symbols

ho	Fluid density [kg/m <sup>3</sup> ]
$\omega$	Angular excitation frequency [rad/sec]
$\omega_1$	Angular pulsation of the reservoir's fundamental mode [rad/sec]
$\omega/\omega_1$	Ratio of the angular frequency of the
	seismic excitation to that of the reservoir's fundamental mode.
k	Bulk modulus of the fluid
$\Phi$	Velocity potential function
$\lambda$	The wavelength
$\sigma$	Surface-wave parameter
CW	Surface-wave parameter
B	Compressibility parameter
S	Total contour of the reservoir boundaries.
$\Omega$	Reservoir domain.
$\Delta$	Laplacian operator; $\Delta = \frac{\partial^2}{\partial x^2} + \frac{\partial^2}{\partial y^2} + \frac{\partial^2}{\partial z^2}$
$\vec{ abla}$	Gradient operator $\vec{\nabla} = (\frac{\partial}{\partial x}, \frac{\partial}{\partial y}, \frac{\partial}{\partial z})$

# GENERAL INTRODUCTION

### GENERAL INTRODUCTION

Dams are vital infrastructure for water supply, energy production, and flood control. However, their safety can be compromised by seismic events, which generate dynamic interactions between the reservoir water and the dam structure. These interactions generate hydrodynamic pressures on the upstream face of the dam, which may significantly impact its stability. Reliable evaluation of these pressures is therefore essential in earthquake engineering and in the design of safe hydraulic structures.

Early analytical studies provided the first foundations for this field. In 1933, Westergaard introduced the concept of added mass, which allowed engineers to estimate hydrodynamic forces by assuming rigid dams and incompressible fluids. Although pioneering, this approach neglected surface-wave effects, dam flexibility, and fluid compressibility. Zangar (1952) and Housner (1957) extended the analysis with electrical analogies and impulsive—convective decomposition, while Chopra (1966) introduced compressibility and derived exact analytical formulations. These works represented significant advances, but they remained limited in their ability to capture all relevant physical effects.

The development of numerical methods in the 1960s and 1970s, especially the Finite Element Method (FEM), marked a turning point. FEM made it possible to represent realistic geometries and boundary conditions and to incorporate effects such as surface gravity waves and fluid compressibility. Despite these advances, many practical analyses continued to neglect surface-wave phenomena, which generally results in conservative (overestimated) hydrodynamic pressures, especially at the dam's top where surface waves can induce negative pressures, accompanied by a reduction of pressure at the base, and most evident at low excitation frequencies.

The present thesis contributes to this ongoing effort by developing a finite element model of a rigid vertical dam—reservoir system in order to quantify the influence of surface waves on hydrodynamic pressures. Beyond this framework, complementary analytical formulations have been developed in collaboration with my supervisor as part of a scientific article currently under review at LARHYSS JOURNAL, titled "EFFECTS OF SURFACE GRAVITY WAVES ON RIGID DAMS." To provide context and enable comparison, selected results from this ongoing analytical research are included in the annex as supplementary material. These annexed results are exclusively illustrative and do not reproduce the full content of the article, which serves as a natural extension of the present work.

#### 0.1 Motivation

Earthquakes can generate significant hydrodynamic pressures on concrete dams, potentially leading to cracking or partial failure. Such failures can have catastrophic downstream consequences, threatening lives, infrastructure, and water resources. Despite progress in seismic design codes, many existing dams were constructed before modern standards and lack reliable

numerical tools to accurately predict their seismic response. Therefore, it is essential to develop advanced numerical models capable of accurately predicting hydrodynamic pressures in the reservoir under both seismic and harmonic excitations while considering the influence of fluid compressibility and surface gravity waves.

#### 0.2 Objectives of the study

This research aims to clarify the effects of surface waves on hydrodynamic pressures in damreservoir systems during seismic events. The specific objectives are :

- 1. Develop a finite element model of the reservoir for both incompressible and compressible fluid cases.
- 2. Analyze surface gravity wave effects under harmonic and seismic loading
- 3. Compare hydrodynamic pressures with and without surface-wave effects
- 4. Identify key parameters influencing surface-wave significance.
- 5. Show conditions where neglecting surface waves impacts seismic safety assessments.

The study focuses on a vertical rigid dam and a horizontal reservoir bottom. It neglects dam deformability and sediment to better isolate hydrodynamic pressures.

#### 0.3 Structure of the dissertation

This dissertation is organized as follows:

- Chapter 1 reviews the historical evolution of hydrodynamic pressure analysis and highlights the role of surface waves.
- Chapter 2 presents the mathematical model and governing equations.
- Chapter 3 describes the finite element implementation and provides comparative numerical results for the Oued El Fodda dam. It contains numerical applications, comparisons, and interpretations of results.
- The General Conclusion summarizes the findings and outlines perspectives for future research.

## PART 1

Background and Literature Review

## CHAPTER 1

LITERATURE REVIEW

### Chapitre 1

#### LITERATURE REVIEW

#### 1.1 Introduction

This chapter reviews the historical development of methods used to analyze hydrodynamic pressures on dams during seismic events. Starting with early analytical approaches such as Westergaard's formulation, we trace the evolution of models and their limitations, including the neglect of fluid compressibility and surface gravity wave effects. We then examine key contributions from Zangar, Housner, Chopra, and others that progressively addressed these shortcomings. Finally, the chapter outlines the transition from simplified analytical formulations to modern numerical techniques such as the Finite Element Method (FEM), which forms the basis of the present study.

#### 1.2 Historical context and major seismic accidents

Most large dams are designed to withstand earthquakes; however, a few accidents have shown how dams can fail. These rare events led engineers to develop more sophisticated analysis methods that now consider dam flexibility, water compressibility, and dynamic effects such as surface gravity waves.

Building on this improved understanding, notable examples such as the 1967 Koyna Dam earthquake in India, which caused structural cracking due to hydrodynamic effects, and the 1999 Chi-Chi earthquake in Taiwan, where the Shih-Kang Dam suffered partial failure [1], further advanced the field. These incidents underscored that simplified models, such as Westergaard's added-mass formulation, could not capture all dynamic effects. In particular, they highlighted the role of dam flexibility, reservoir bottom absorption, and surface wave generation, all of which are best addressed within a finite element modeling framework.

These historical analyses and the lessons from major dam failures motivate the detailed review of classical analytical models and their limitations presented in the following sections.

#### 1.3 Classical analytical and semi-analytical approaches

The foundation for modern hydrodynamic pressure analysis lies in classical analytical models. These can be traced through the following key contributions:

#### 1.3.1 Early pioneers and their fundamental assumptions

The first analytical models aimed to provide explicit, closed-form solutions for engineering applications. Although pioneering, these models depended on rigid assumptions that constrained their reliability under actual seismic conditions.

#### 1.3.1.1 Westergaard's simplified model (1933)

Westergaard (1933) introduced the first practical formulation of hydrodynamic pressures acting on a rigid, vertical dam subjected to horizontal ground motion. His approach, known as the added mass method, treats the hydrodynamic effect as an inertial force arising from a fictitious mass of water that moves with the dam. This concept simplifies the fluid-structure interaction to an equivalent structural inertia problem [2, 3, 4, 5, 6].

The classical formulation is based on several key assumptions:

- The reservoir water is incompressible and inviscid.
- Surface wave effects at the free surface are neglected.
- The dam is modeled as a rigid body with an infinite upstream reservoir length.
- Only the fundamental mode of horizontal excitation is considered.

Westergaard's solution is applicable primarily when the excitation frequency is below the fundamental frequency of the reservoir [4, 5]. Despite its simplicity, the method remains widely used in the preliminary seismic design of gravity dams, where low-frequency excitation dominates and water is often assumed incompressible [4, 7, 8].

However, this approach tends to overestimate hydrodynamic pressures because it neglects significant factors such as dam flexibility and surface wave generation. This motivated subsequent researchers, starting with Zangar, to extend and refine the theory.

Although not a numerical method itself, the added mass concept has been incorporated into many finite element and numerical techniques [4]. For example, Mir & Taylor (1995) applied the concept in experimental settings to approximate dam-reservoir pressures [4]. Nonetheless, it remains recognized that the original formula often overpredicts maximum pressures, leading to the proposal of correction factors that account for dam elasticity, reservoir geometry, and sediment presence.

Despite these limitations, Westergaard's formulation is foundational, still forming the basis of many design codes and guidelines. It may be regarded as a special case within more generalized models that include compressibility, surface gravity waves, and flexibility [4].

In the decades following Westergaard's publication, further developments arose. Researchers in the 1950s and 1960s systematically addressed these limitations by developing more advanced models. Beginning with Zangar's electrical analogies, Housner's impulsive-convective decomposition, and Kotsubo's extensions accounting for earthquake motion randomness. These lay the groundwork for modern numerical and analytical methods, which are further elaborated in the next chapters.

#### 1.3.1.2 Zangar electrical analogy method (1952)

Building on Westergaard's simplified model, Zangar (1952, 1953) developed an electrical analogy method and was the first to experimentally investigate the influence of the upstream face geometry of dams. He showed that hydrodynamic pressures are consistently smaller for dams with non-vertical faces. These findings provided crucial validation data for later analytical and numerical models [7, 9].

#### 1.3.1.3 von Kármán and Housner (1957)

Housner idealized the liquid as incompressible and posed and solved the problem in an approximate and simple way with acceptable results. To do this, he decomposed the motion into impulsive and oscillatory. He applied the results to rectangular, cylindrical, and elliptical tanks and to rigid inclined walls and studied the effect of the dam's flexibility. He demonstrated that hydrodynamic pressures decrease as the dam's flexibility increases, an insight later verified with numerical models. [10]

#### 1.3.1.4 Kotsubo (1960)

Kotsubo challenged the validity of the added-mass approach by emphasizing that earthquakes are inherently random and cannot be represented adequately by simplified harmonic excitation [11]. He showed that maximum dynamic pressures can be considerably larger than those predicted by Westergaard's equation [12].

Importantly, Kotsubo demonstrated that dynamic water pressure is not always proportional to ground acceleration. When the earthquake period is shorter than the reservoir's resonance period, the pressure response lags the acceleration phase by about 90°, acting as a damping force that may, in some cases, enhance dam safety [12].

He also provided one of the first theoretical solutions for the three-dimensional distribution of dynamic pressures in arch dams, an important step toward treating more complex dam geometries [12].

## 1.3.1.5 Anil K. Chopra (1966): hydrodynamic pressures on dams during earthquakes

Chopra was one of the first researchers to systematically investigate the limitations of classical hydrodynamic formulations for dams under seismic loading. His seminal 1966 report[13] sought to determine accurate hydrodynamic pressures acting on dams during real earthquake motions, moving beyond simplified design approaches such as Westergaard's "virtual mass" method. Chopra's objective was to establish a rigorous analytical framework that incorporated the inherently dynamic and complex nature of earthquake excitations. Chopra's model incorporated several critical assumptions:

- Dam and Reservoir Geometry: A vertical, rigid dam face with an infinitely long reservoir in the upstream direction.
- Fluid Properties: Water was modeled as a compressible, inviscid (ideal), and initially still fluid. Compressibility was a central and novel aspect of his study.
- Excitation: Both horizontal and vertical components of ground motion were analyzed, with the 1940 El Centro earthquake used as the primary input.

A key aspect of Chopra's research was to evaluate the necessity of including surface waves at the free surface boundary condition (y = H). Two boundary conditions were compared:

Exact Boundary Condition (including surface waves):

- Exact Condition (with surface waves):

$$\frac{\partial^2 \Phi}{\partial t^2} + g \frac{\partial \Phi}{\partial y} = 0 \tag{1.1}$$

Where  $\Phi$  is the velocity potential

- **Simplified Condition** (without surface waves) :

$$p = 0 (1.2)$$

Justification for Simplifying or Neglecting Surface gravity Waves:

- Horizontal Motion: Referencing Bustamante et al.[10], Chopra employed an error criterion based on the dimensionless parameter H/T. His analysis showed that for typical earthquake frequencies, the error in neglecting surface waves is less than 5%, supporting the use of the simplified boundary condition.
- Vertical Motion: Chopra performed calculations with and without the full surface wave condition. He found only negligible differences between the two solutions, concluding that the simplified condition p = 0 "is sufficiently accurate for engineering purposes."[13]

#### 1.3.1.6 Nath (1969)

Nath (1969) extended the analysis of hydrodynamic pressures using the finite element method, focusing particularly on vertical ground motions for both vertical and inclined dam faces. His work provided important refinements to earlier studies, including Chopra's.[13].

Nath actually **confirmed and reinforced** Chopra's finding that surface wave effects are generally negligible for seismic analysis. He demonstrated quantitatively that:

$$n = \frac{cT}{H} \tag{1.3}$$

For high frequencies (e.g., n=30), the difference between applying the linearized free-surface condition and simply taking p=0 at the surface was minimal—the pressure coefficient at the free surface was only 0.0002 in the former case versus zero in the latter. Nath concluded that "surface gravity waves would have some effect on dynamic pressures only when the relative frequency of motion is very small, and that for relatively high frequencies—where compressibility effects become significant—the simplified condition p=0 at the free surface is sufficiently accurate."

Nath's significant contributions included:

- Developing one of the earliest **finite element applications** to dam-reservoir interaction problems
- Providing numerical validation of compressibility effects for complex geometries, including inclined dam faces
- Showing that inclined dams experience **lower pressure coefficients** than vertical dams
- Demonstrating that pressure distribution varies with reservoir length for inclined dams, unlike vertical dams where pressures remain constant along the reservoir

His work represented an important transition toward numerical methods in dam engineering, providing the framework for more sophisticated finite element and boundary element formulations that would follow.[14]

#### 1.3.2 Limitations of classical approaches

While classical analytical methods provided foundational insights into hydrodynamic pressures, they were constrained by several significant simplifications that limited their accuracy for complex seismic analysis.

The most notable limitation was the treatment of the free surface condition. Methods like Westergaard neglect surface-wave effects by assuming (p = 0 at y = H), neglecting the dynamic interaction between surface waves and hydrodynamic pressures. However, subsequent research by Chopra [13] and Nath [14] demonstrated that this simplification was actually **justifiable** for high-frequency seismic analysis, as surface wave effects were quantitatively shown to be negligible (approximately 5% error) for the dominant frequencies in earthquake excitations.

The more critical limitation emerged in the treatment of water compressibility. Classical approaches either:

- Assumed incompressible water (e.g., Zangar's method), leading to errors of 20-51% in peak pressure estimates
- Were restricted to harmonic excitations with periods longer than the reservoir's fundamental period (e.g., Westergaard's method)

Additionally, these methods could not adequately handle:

- Complex dam geometries (e.g., inclined faces, arch dams)
- Three-dimensional reservoir effects
- Dam-reservoir-foundation interaction
- Arbitrary earthquake time histories with wide frequency content

The **virtual mass concept** proved particularly problematic, as it became invalid when excitation periods approached the reservoir's resonant periods, where phase differences between acceleration and pressure become significant.

These limitations highlighted the necessity for more sophisticated approaches that could properly account for water compressibility, complex geometries, and full dynamic interaction—ultimately driving the development of numerical techniques such as the finite element method (FEM) and boundary element method (BEM). These limitations provided the impetus for the development of more advanced numerical methods, notably the finite element method, discussed in the following subsection.

#### 1.3.3 Development of numerical methods

The advent of digital computers in the 1960s and 1970s enabled the use of numerical methods for dam—reservoir interaction analysis. These approaches overcame many of the limitations of classical analytical models by explicitly incorporating water compressibility, dam flexibility, complex geometries, and surface gravity wave effects.

Chopra and his colleagues made pioneering contributions by formulating finite element procedures that included reservoir geometry and water compressibility [4]. Their work showed that Westergaard's solution is valid only when the excitation frequency is less than the fundamental frequency of the reservoir, and that water may be treated as incompressible if the dam's fundamental frequency is less than half that of the reservoir [4, 5].

To reduce computational cost, Chakrabarti and Chopra [4] developed a boundary element method (BEM), which required discretization only of the reservoir boundaries. Later, Hall and Chopra (1982) proposed a two-dimensional FEM procedure for the dynamic analysis of concrete gravity dams, treating the dam as elastic and the water as compressible. Fenves and Chopra (1984, 1987) further refined these methods to include dam–water–foundation interaction and reservoir bottom sediments.

Other significant contributions include Sharan (1985), who extended FEM to handle complex geometries and introduced a technique for modeling radiation damping in infinite reservoirs. His numerical results compared favorably with analytical solutions derived by Chwang [7, 9].

In the 1980s and 1990s, these advances laid the foundation for more sophisticated computational methods. Recent developments include coupled FEM-BEM techniques, scaled boundary FEM,

and mesh-free methods such as smoothed particle hydrodynamics (SPH). These approaches offer improved computational efficiency, higher accuracy, and better treatment of surface waves and nonlinear effects, making them well-suited for dam—reservoir interaction studies.

## 1.4 Integration of surface wave effects in dam–reservoir analysis

The influence of surface waves on hydrodynamic pressure distribution has long been recognized, yet these effects are often neglected in practical analyses. This is mainly because classical analytical methods neglect the wave motion at the free surface, while early numerical models prioritized computational efficiency over free-surface accuracy. As a result, most design-oriented studies overestimated surface-wave contributions.

A more complete treatment of dam-reservoir system, therefore, requires explicit integration of surface waves into numerical formulations, an approach that has only recently become practical with advances in computational power and modeling techniques.

## 1.4.1 Bustamante et al. (1963): free-surface and compressibility effects

Bustamante, Rosenblueth, Herrera, and Flores presented a comprehensive theoretical analysis of hydrodynamic pressures on dams during earthquakes [10]. Their study formulated the dam–reservoir interaction problem for a compressible, inviscid, and irrotational fluid under small displacements, excited by harmonic ground motion.

The governing equation reduces to a wave equation for the velocity potential  $\omega$ :

$$\frac{\partial^2 \omega}{\partial x^2} + \frac{\partial^2 \omega}{\partial y^2} - \frac{\gamma_0}{gE_v} \frac{\partial^2 \omega}{\partial t^2} = 0, \tag{1.4}$$

where  $E_v$  is the bulk modulus of water,  $\gamma_0$  the unit weight, and g gravity.

The free-surface boundary condition is given by:

$$\frac{\partial^2 \omega}{\partial t^2}(x, H, t) + g \frac{\partial \omega}{\partial u}(x, H, t) = 0, \tag{1.5}$$

which fully accounts for surface gravity waves (seiches). Because solving this exactly is difficult, a common simplification sets  $\omega(x, H, t) = 0$ , effectively neglecting surface waves.

### **1.4.1.0.1 Key findings.** The authors quantified the errors introduced by common simplifications :

- 1. Neglecting surface waves:
  - Error in hydrodynamic force Q is < 5% when  $\frac{H}{T} > 4.2\sqrt{H}$ ,
  - Error is < 20% when  $\frac{H}{T} > 2.6\sqrt{H}$ .
- 2. Neglecting compressibility:

- Small errors for  $\frac{H}{T}$  < 100 m/s,
- Very large errors (up to 100%) near resonance at  $\frac{H}{T} \approx 359.6$  m/s.
- 3. Reservoir length-to-depth ratio (L/H):
  - For L/H > 5, results converge to those of an infinite reservoir,
  - For  $L/H \approx 1$ , significant differences occur, especially above the first critical frequency.

**1.4.1.0.2** Implications. This study provided one of the first rigorous formulations of the dam—reservoir problem with compressibility and surface wave effects. It demonstrated that while surface waves can sometimes be neglected for high-frequency motions, they become crucial at low frequencies and for short reservoirs, reinforcing the need for numerical approaches capable of capturing these effects.

## 1.4.2 Chwang (1981, 1985) : Surface waves, compressibility, and flexibility

The impact of surface gravity waves on hydrodynamic pressure distribution was a key area of Chwang's research [7]. In a 1981 study, Chwang [15] performed a perturbation analysis to investigate the effect of density stratification in the reservoir fluid. Specifically, he examined how a linear density profile,  $\bar{\rho}(y) = \rho_0(1-\epsilon y/h)$ , modifies the hydrodynamic pressure. Although stratification was the primary focus, the analysis was conducted within the framework of linear wave theory, which inherently includes surface waves. The wave-effect parameter  $C = g/(\omega^2 h)$  appeared as a fundamental quantity, and the resulting pressure distribution included both inphase and out-of-phase components, the latter arising directly from the free-surface boundary condition.

Chwang's subsequent report with Huang [16] marked a major advance. This work presented a comprehensive general method for analyzing three-dimensional reservoirs of arbitrary planform. Surface wave effects (parameter C) were treated explicitly and on equal footing with water compressibility (parameter  $B = \omega h/c_0$ ) and reservoir geometry. The study demonstrated that when C > 0, the pressure distribution becomes oscillatory near the free surface, a radical departure from classical solutions.

The 1985 study also extended the formulation to flexible dams by representing the dam-face motion as a superposition of modal shapes. This revealed how structural flexibility interacts with reservoir hydrodynamics, significantly altering both pressure distributions and system resonance characteristics.

Together, these contributions established a systematic framework for including surface waves, compressibility, and flexibility in dam–reservoir interaction analysis, paving the way for later FEM and BEM implementations.

## 1.4.3 Eatock Taylor (1981) : mode superposition and surface wave criteria

Eatock Taylor reviewed the analysis of hydrodynamic loads on submerged structures such as dams, intake towers, and offshore platforms during seismic events [5]. A central theme of his

work was the dynamic interaction between fluid loading and structural response. To illustrate key physical effects, he presented an analytical solution for a simplified two-dimensional damreservoir system, explicitly accounting for fluid compressibility and free-surface motion.

The method proceeds in two steps. First, the structure is analyzed in a "dry" state (without fluid) to determine its natural vibration modes and frequencies. Second, the influence of the surrounding fluid is superimposed onto these dry modes using modal analysis, avoiding the need to solve the fully coupled fluid-structure system simultaneously. This mode superposition approach reduces computational effort while capturing essential hydrodynamic effects.

The hydrodynamic pressure p(x, y, t) is expressed as a linear superposition of contributions from ground motion and the structure's vibration modes. The governing equation for the unit pressure function  $\theta_r$  (which defines the pressure distribution per mode) is the modified Helmholtz equation:

$$\nabla^2 \theta_r = -\frac{\omega^2}{c^2} \theta_r,\tag{1.6}$$

where  $\omega$  is the excitation frequency and c is the acoustic wave velocity in the fluid.

At the free surface (y = H), the boundary condition incorporates gravity effects:

$$\frac{\partial \theta_r(x,H)}{\partial y} = \frac{\omega^2}{q} \,\theta_r(x,H),\tag{1.7}$$

which shows that surface response depends on both excitation frequency and gravitational acceleration.

From this formulation, Eatock Taylor derived practical criteria for simplifying analyses : Surfacewave effects are negligible when :

$$\omega_1 > 8.3\sqrt{\frac{g}{H}},\tag{1.8}$$

where  $\omega_1$  is the dam's fundamental frequency (in rad/s). This criterion is based on the work by Bustamente et al.[10]. - Compressibility effects are negligible when (following Chopra, 1968):

$$\omega_1 < \frac{\pi c}{4H}.\tag{1.9}$$

Importantly, these two conditions overlap only for extremely deep reservoirs (H > 1890 m). For most practical dam heights, either compressibility or surface wave effects (or both) must be considered to ensure accurate seismic analysis.

#### 1.4.4 Wu and Yu (1989): Trefftz method and wave–Dam interaction

Wu and Yu employed the Trefftz method to analyze the influence of surface gravity waves on hydrodynamic pressure distributions along rigid dams with non-vertical upstream faces [9]. Their approach used a set of T-complete functions that satisfied the Laplace equation and all boundary conditions except on the dam face, where a least-squares fit was applied.

They introduced the wave-effect parameter

$$CW = \frac{g}{\omega^2 H},\tag{1.10}$$

and showed that hydrodynamic pressure decreases as CW increases, attributing this effect to energy radiated away by propagating surface waves.

Their numerical results, computed with 25 series terms, were compared with Chwang's exact solutions (which neglected surface waves) and with Zangar's experimental data. The agreement was good, and the study highlighted the significance of wave effects—especially for dams with sloped upstream faces. Wu and Yu's work remains a key reference in numerical investigations of wave–dam interaction under seismic conditions.

#### 1.4.5 Tsai and Wei (1991)

Tsai and Wei investigated the hydrodynamic pressure on an oscillating vertical plate. They reported that compressibility is effective at higher oscillation frequencies in deep reservoirs, with pressures exceeding those of incompressible fluids, particularly near the bottom. At lower frequencies, the effect of surface waves was more significant, producing negative pressures close to the free surface. Experiments were also performed to examine the wave effect, and the results showed good agreement with theoretical studies.[17]

#### 1.4.6 Martin (1992): wavemaker analogy and surface wave criteria

Martin revisited the hydrodynamic problem of dams under seismic loading by drawing an analogy with Havelock's classical wavemaker problem [18]. His analysis emphasized the role of surface waves, which had often been neglected in earlier dam-reservoir models.

In the wavemaker problem, surface waves are explicitly included through the free-surface boundary condition,

$$K\phi + \frac{\partial \phi}{\partial y} = 0$$
 on  $y = 0$ , (1.11)

where  $K = \omega^2/g$ , and  $\phi$  is the velocity potential. This condition admits propagating gravity waves, with the fundamental eigenfunction

$$\phi_0(x,y) = e^{ik_0x} Y_0(y), \tag{1.12}$$

where  $k_0$  satisfies the dispersion relation

$$K = k_0 \tanh(k_0 h). \tag{1.13}$$

This formulation captures both radiating surface waves and higher-order evanescent modes, placing surface waves at the center of the analysis.

By contrast, Martin reformulated the dam problem as the limiting case  $K \to \infty$ , corresponding to short-duration earthquake loading where gravitational effects are negligible. In this regime, the free-surface condition becomes

$$\phi(x,0) = 0, \quad x > w(0), \tag{1.14}$$

so that no surface gravity waves are generated. This distinction clarified that surface waves are essential for long-duration or harmonic excitations, but can be neglected under impulsive loading conditions.

Martin further demonstrated that for both vertical and non-vertical wavemakers (or dams), the velocity potential can be represented as a convergent eigenfunction expansion—provided the geometry satisfies specific constraints. By adapting the Rayleigh hypothesis from acoustics, he identified the allowable shapes for which such an expansion remains valid everywhere in the fluid, thus extending Westergaard's classical solution to more general dam faces.

## 1.4.7 Maity and Bhattacharya (1999, 2003): boundary conditions for FEM with surface waves

Maity and Bhattacharya [3] introduced an efficient far-boundary condition for truncating the infinite reservoir domain in finite element models. Their formulation treated pressure as the nodal variable and incorporated fluid compressibility, enabling time-domain analyses of damreservoir systems. A key advantage was that the artificial boundary could be placed relatively close to the structure without compromising accuracy, thereby reducing computational cost. For dams with vertical upstream faces under steady-state loading, their approach produced results in close agreement with classical solutions, even when the truncation surface was set at a short distance from the dam. Importantly, the free-surface boundary condition in their method explicitly included the effects of surface waves.

Building on this work, [2] They developed a more general FEM procedure for coupled fluid-structure systems, again assuming a compressible, inviscid fluid with pressure as the unknown variable. Their extended formulation retained the explicit treatment of surface waves, making it applicable to a broader range of dynamic loading problems.

Together, these contributions provided a practical and computationally efficient FEM framework for dam—reservoir interaction that overcame one of the main challenges in numerical modeling: representing the infinite reservoir while still accounting for compressibility and surface wave effects.

## 1.4.8 Attarnejad and Zahedi (2004): time-domain exact solution with surface waves

Attarnejad and Zahedi presented a time-domain exact solution for the coupled response of gravity dams and reservoirs, explicitly accounting for surface wave effects [6]. Their analysis assumed an incompressible and irrotational fluid and demonstrated that hydrodynamic pressures can be significantly larger when surface waves are included—up to three times greater than those predicted under the assumption of a fixed free surface.

This result highlights the critical role of free-surface motion in seismic dam analysis and provides strong evidence that neglecting surface waves can lead to unsafe underestimation of hydrodynamic loads. Their work, therefore, underscores the need to integrate surface wave effects into modern numerical approaches.

## 1.4.9 Avilés and Suárez (2010) : surface waves in compressible and viscous fluids

Avilés and Suárez extended the Trefftz method to investigate the effects of surface gravity waves on the hydrodynamic pressures of rigid dams with arbitrary upstream faces, while also accounting for water compressibility and viscosity [7]. Their formulation used a complete set of Trefftz functions that satisfied the reduced wave equation and all boundary conditions except on the dam face, where the solution was determined in the least-squares sense.

They characterized the surface wave effect using the parameter

$$\sigma = \frac{\omega^2 H_r}{q},\tag{1.15}$$

and found that hydrodynamic pressures are significantly influenced by surface waves for values of  $\sigma < 10$ , but become irrelevant for large values (e.g.,  $\sigma = 100$ ).

Their results showed that surface waves generate negative pressures at the dam's top and reduce positive pressures at the base, with the former effect being more critical for fully inclined faces. They concluded that while the influence of surface waves is distinct, it is generally smaller than the effect of internal waves from fluid compressibility, which dominate at the reservoir's resonant frequencies. The study provided a comprehensive closed-form solution, validating its convergence and accuracy against existing exact solutions for both vertical and sloping dams.

## 1.4.10 Gogoi and Maity (2006–2010): truncation boundaries and frequency-domain approaches

Gogoi and Maity in 2006 introduced a new truncation boundary condition for evaluating hydrodynamic pressures in infinite reservoirs [4]. This formulation incorporated the absorptive properties of the reservoir bottom and the reflection coefficient of sedimentary layers, making it suitable for unbounded domains in FEM applications.

In 2007, they extended this framework by explicitly including surface wave effects in the freesurface boundary condition. Their formulation assumed an inviscid, irrotational, and linearly compressible fluid subjected to small-amplitude motion, further enhancing the physical realism of dam—reservoir interaction models.

Later, in 2010 they proposed a short-term Fourier transform (STFT)-based solution for dynamic dam—reservoir problems, allowing the identification of frequency-dependent interactions at the reservoir bottom. This frequency-domain approach provided a flexible tool for analyzing complex bottom boundary conditions and transient seismic inputs.

Taken together, these contributions advanced the numerical modeling of dam—reservoir systems by integrating surface wave effects with more realistic boundary conditions, bridging the gap between idealized theory and practical FEM implementations.

## 1.4.11 Pani and Bhattacharyya (2008): FEM with free-surface and truncated boundaries

Pani and Bhattacharyya investigated the hydrodynamic pressure on a vertical rectangular gate using the finite element method (FEM), treating fluid pressure and gate displacement as independent nodal variables. Their formulation incorporated a linearized free-surface condition to represent surface waves—justified by the small amplitude of waves relative to the fluid depth, despite the inherently nonlinear nature of free-surface flows—and a near-truncation boundary condition to efficiently approximate the unbounded reservoir.[19]

## 1.4.12 Chen and Yuan (2011); Abdollahi and Attarnejad (2012): quantifying surface wave effects

Chen and Yuan and Abdollahi and Attarnejad emphasized the role of surface waves in dam–reservoir interaction. Their studies showed that surface-wave effects can augment hydrodynamic pressures by up to 10% in linear analyses and become even more significant under ramp-type seismic excitations [20, 21].

#### 1.4.13 da Silva and Pedroso (2019)

da Silva and Pedroso developed an analytical solution in the complex plane to study the damreservoir interaction problem for a rigid dam and a semi-infinite, incompressible fluid reservoir [22]. Their formulation solved the Laplace equation to determine the hydrodynamic pressure field, explicitly incorporating the effects of surface gravity waves through a linearized free-surface boundary condition. A key outcome of their work was the derivation of the complex hydrodynamic force on the dam, which they separated into a conservative part (real component), representing the inertial added mass effect, and a dissipative part (imaginary component), quantifying the energy radiated away from the structure by surface waves.

They demonstrated that the balance between these inertial and radiative effects is governed by the **Froude number**  $(F_r)$ , a dimensionless parameter they defined as the square of :

$$F_r^2 = \frac{\omega^2 H}{g} \tag{1.16}$$

where  $\omega$  is the excitation frequency, H is the reservoir depth, and g is the acceleration due to gravity. Their analysis showed that the dissipative effect decreases as the Froude number increases, while the conservative effect increases. The study also provided asymptotic solutions for both very low and very high Froude numbers, offering simplified expressions for these limiting cases.

In summary, this work provided a fundamental analytical framework that clearly isolates and characterizes the mechanisms of energy dissipation due to **surface wave radiation** in damreservoir systems, complementing numerical approaches by offering exact benchmark solutions. Despite such findings, many practical analyses continue to neglect free-surface motion due to the added computational complexity. Addressing this gap requires numerical models that can efficiently incorporate surface-wave effects. The present work contributes to this effort by employing a finite element model with a Neumann boundary condition at the free surface, offering a framework that balances accuracy with computational feasibility [7].

In summary, while classical analytical models laid the groundwork for understanding damreservoir interactions, their simplifying assumptions limited their applicability to modern dams and loading conditions. Progressing from these foundations, this thesis adopts a finite element framework that incorporates both fluid compressibility and surface-wave effects, providing an advanced tool for accurate seismic analysis.

#### 1.5 conclusion

This chapter has traced the historical development of methods for analyzing hydrodynamic pressures on dams, beginning with classical analytical approaches and progressing to modern numerical formulations. Early studies established the fundamental concepts of added mass and rigid-reservoir assumptions, but they also introduced significant simplifications, most notably, the neglect of water compressibility, dam flexibility, and free-surface motion. Subsequent research progressively relaxed these assumptions, incorporating compressibility and geometry effects, and demonstrating that surface waves can strongly influence hydrodynamic pressures.

Despite these advances, surface-wave effects remain frequently overlooked in practical engineering analyses, largely due to their computational complexity. The literature reviewed in this chapter shows that neglecting them can lead to a substantial overestimation of hydrodynamic pressures.

The next chapters build directly on these insights by developing a finite element framework for a rigid vertical dam—reservoir system. This model explicitly incorporates surface-wave effects through appropriate free-surface boundary conditions, providing a more realistic assessment of hydrodynamic pressures under seismic loading.

## PART 2

Theoretical Framework and Mathematical Formulation

## CHAPTER 2

MATHEMATICAL MODEL GOVERNING EQUATIONS

### Chapitre 2

# MATHEMATICAL MODEL AND GOVERNING EQUATIONS

#### 2.1 Introduction

To establish the mathematical framework for this work, this chapter formulates the governing equations of the dam—reservoir system. Emphasis is placed on hydrodynamic pressures exerted on a rigid vertical dam, with explicit distinction between compressible and incompressible fluid models. The formulation is developed for numerical implementation using the Finite Element Method (FEM), as introduced in Chapter 1. We begin with the geometric assumptions of the dam—reservoir system, followed by the governing equations of fluid motion. Finally, the relevant boundary conditions are derived, including the treatment of the free surface with and without surface—wave effects.

#### 2.2 Modeling assumptions and geometry

The reservoir is assumed to have **constant depth** (H) and a **rigid horizontal bottom**. Its length is considered sufficiently large to approximate an infinite domain, which is typically satisfied for  $L \geq 3H$  in practical FEM applications, where L denotes the length of the computational domain. These geometric simplifications underpin the following analysis.

Building upon these assumptions, we consider a vertical dam subjected to horizontal ground acceleration, denoted as  $\ddot{u}_n$ , as illustrated in Figure 2.1. The coordinate origin is placed at the base of the reservoir. Due to the dam's rigidity, all points along the dam-fluid interface experience the same acceleration as the base. The dam-reservoir system is modeled in two dimensions, with the following fluid assumptions: the water is linearly compressible, inviscid, and irrotational. For the purposes of this simplified seismic analysis, the **peak ground acceleration** is assumed to fully characterize the seismic input and is used to define the relevant seismic parameters [23].

#### 2.2.1 Geometry and computational domain

As depicted in Figure 2.1, the reservoir is modeled as a rectangular domain  $\Omega$  bounded by four distinct boundaries :

- $\mathbf{S}_1$ : The impermeable bottom of the reservoir (y=0).
- $\mathbf{S}_2$ : The truncated lateral boundary at the far end of the reservoir (x = L).
- $S_3$ : The free surface of the water (y = H)
- $\mathbf{S}_4$ : The vertical dam-reservoir interface  $(x = 0, 0 \le y \le H)$ .
- Total Boundarys :  $S = S_1 \cup S_2 \cup S_3 \cup S_4$

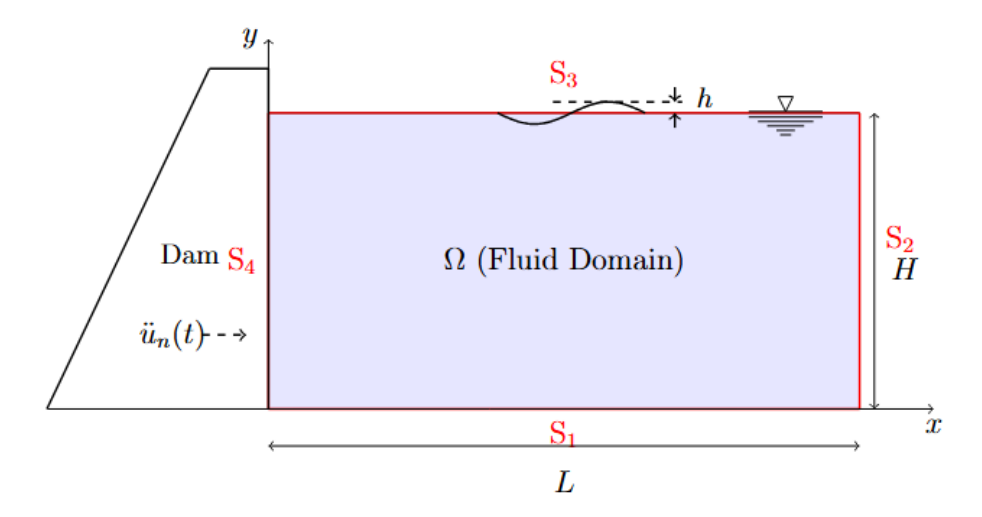


Figure 2.1: Geometry of the dam-reservoir system

#### 2.3 Theoretical formulation

#### 2.3.1 Governing equations for fluid

Building on the modeling assumptions introduced in Section 2.2, we make the following additional simplifications for the derivation of the governing equations:

- (a) the reservoir is considered infinitely long in one direction, allowing a two-dimensional formulation;
- (b) fluid motions are assumed to be of small amplitude, justifying linearization of the governing equations.

Under these assumptions, and considering the reservoir water to be linearly compressible and inviscid, the Navier–Stokes equation expressing the dynamic balance of fluids reduces to:

$$\rho \dot{\mathbf{v}} = -\nabla p \tag{2.1}$$

p is the hydrodynamic pressure in the liquid and  $\rho$  the mass density of water. For a complete description, the mass conservation equation as well as the equation of state must be combined with the preceding equation of motion [24]. They are written, respectively, as

$$\dot{\rho} + \rho \nabla \mathbf{v} = 0 \tag{2.2}$$

The relationship between the fluid density and the resulting hydrodynamic pressure is defined by the equation of state :

$$d\rho = \frac{\rho}{k}\dot{p} \tag{2.3}$$

Where k the fluid's bulk modulus. From equations 2.2 and 2.3, we can write:

$$\frac{\rho}{k}\dot{p} + \rho\nabla \mathbf{v} = 0 \tag{2.4}$$

Multiplying equation 2.4 by  $\nabla$  and differentiating equation 2.3 with respect to time leads to the following system of dynamic equilibrium equations:

$$\rho \nabla \dot{\mathbf{v}} + \nabla^2 p = 0 \tag{2.5}$$

$$\rho \nabla \dot{\mathbf{v}} + \frac{1}{C^2} \ddot{p} = 0 \tag{2.6}$$

Where :  $C = \sqrt{k/\rho}$  denotes the acoustic wave velocity in water. For water,  $C \approx 1438$  m/s. Eliminating the variable v from the system of equations 2.5 and 2.6 leads to the wave equation governing the behavior of the pressure perturbation inside the reservoir:

$$\nabla p^2 + \frac{1}{C^2}\ddot{p} = 0 \tag{2.7}$$

In the incompressible limit  $(C \to \infty \Rightarrow k \to 0)$ , (Eq. 2.7) reduces to Laplace's equation.

$$\nabla^2 p = 0 \tag{2.8}$$

For a compressible fluid, the equation that governs the problem is none other than the Navier-Stokes equation with all its terms: The dam is modeled as a rigid body undergoing base excitation, expressed as

$$\ddot{u}_n(t) = e^{i\omega t} \tag{2.9}$$

Where : w is the circular frequency of vibration. This formulation allows us to later apply the Finite Element Method (see Chapter 3) to capture the dynamic pressure distribution. To solve the Helmholtz equation, we define the appropriate boundary conditions, presented in the next section.

#### 2.3.2 Boundary conditions

Boundary conditions are crucial for solving the governing equations, as they specify the behavior of the fluid at the domain boundaries. The boundary conditions for the dam-reservoir system shown in Figure 2.1 are given by :

1. On the upstream face of the dam  $(S_4)$ : At the dam-reservoir interface  $S_4$ , the fluid bonds perfectly to the rigid dam wall. Therefore, the fluid's normal acceleration must equal the dam's prescribed horizontal acceleration,  $\ddot{u}_n$ . The condition can be written in terms of the hydrodynamic pressure gradient as

$$\left. \frac{\partial p(x,y,t)}{\partial n} \right|_{S_4} = -\rho \ddot{u}_n \tag{2.10}$$

where  $\mathbf{n}$  is the outwardly directed normal to the elemental surface along the interface.

2. At the free surface  $(S_3)$ : On the free surface  $S_3$ , the simplest condition is to consider atmospheric pressure p = 0 and to neglect surface waves. However, pressure variations inside the reservoir induce fluctuations of the free surface. [24]

An approximate idea to include the effects of surface waves consists in considering a mean free surface for which any elevation or lowering of the actual surface by a height h (as illustrated in Figure 2.1)results in a pressure variation assumed to be hydrostatic [24]:

$$p = \rho g h \tag{2.11}$$

The dynamic equation applied to this case gives:

$$\frac{\partial p}{\partial n} = -\rho \ddot{h} \tag{2.12}$$

where  $\frac{\partial p}{\partial n}$  is the pressure gradient normal to the free surface, and  $\ddot{h}$  is the second time derivative (acceleration) of the free surface elevation.

Taking twice the time derivative of equation (2.11) and substituting into equation (2.12) yields the linearized free surface wave boundary condition:

$$\frac{\partial p}{\partial n} = -\frac{1}{g}\ddot{p} \tag{2.13}$$

This condition expresses that the normal pressure gradient at the free surface is proportional and opposite to the second time derivative of the pressure. It is known as the linearized free surface boundary condition and is essential to incorporate the dynamic effects of surface gravity waves in hydrodynamic pressure modeling. Under the assumption of small-amplitude waves, the free surface remains nearly horizontal, so the outward normal vector  $\mathbf{n}$  to  $S_3$  is approximately vertical and coincides with the y-axis. Accordingly, the normal derivative reduces to:

$$\frac{\partial p}{\partial y} = -\frac{1}{g}\ddot{p} \tag{2.14}$$

The linearized free surface boundary condition is therefore expressed as

$$\frac{1}{g}\ddot{p} + \frac{\partial p}{\partial y} = 0 \quad \text{(in the Time domain)} \tag{2.15}$$

This expression is referred to as *Poisson's boundary condition* for gravity waves [7]. As previously advanced, the pressure in the reservoir can be given in the frequency domain as:

$$p(x, y, t) = p(x, y, w)e^{i\omega t}$$
(2.16)

we derive the condition in the frequency domain. So, the boundary condition in terms of physical pressure is written as :

$$\frac{\partial p}{\partial y}\Big|_{S_3} = \frac{\omega^2}{g}p$$
 (linearized and in the frequency domain) (2.17)

3. The radiation condition  $(S_2)$ :

This boundary is considered the truncation limit of the domain bounding the reservoir where pressures are completely dissipated. Therefore:

$$p\big|_{S_2} = 0 \tag{2.18}$$

4. At the bottom of the reservoir  $(S_1)$ : This boundary condition, applied at the bottom of the reservoir  $(S_1)$ , which is considered rigid and horizontal, assumes that the fluid particles are perfectly bonded to the solid particles of the dam. As a result, their velocity in the vertical direction is considered to be zero:

$$\frac{\partial p}{\partial y}\big|_{S_1} = 0 \tag{2.19}$$

In summary, the mathematical formulation of the system, taking into account the boundary conditions, is :

$$\begin{cases} \nabla^2 p = \frac{1}{C^2} \frac{\partial^2 p}{\partial t^2} & \text{in } \Omega \\ \frac{\partial p}{\partial n} = -\rho \ddot{u}_n & \text{on } S_4 \\ \text{on } S_3 : \begin{cases} p = 0 & \text{(without surface wave)} \\ \frac{\partial p}{\partial y} = \frac{\omega^2}{g} p & \text{(with surface wave)} \end{cases} \\ p = 0 & \text{on } S_2 \\ \frac{\partial p}{\partial y} = 0 & \text{on } S_1 \end{cases}$$
 (2.20)

#### 2.4 Conclusion

Selecting an appropriate mathematical model is a demanding task that requires careful evaluation by the design engineer. It involves defining calibration parameters, establishing the governing equations for the phenomenon under study, and selecting numerical tools and boundary conditions that closely match real-world behavior. Unlike earlier approaches that overlooked the influence of surface gravity waves on hydrodynamic pressure distribution, this study explicitly accounts for the influence of surface gravity waves through the adopted governing equations and boundary conditions, ensuring a more realistic representation of the hydrodynamic behavior within the reservoir. The resulting formulation establishes a consistent theoretical basis for analyzing the pressure field in the dam—reservoir system.

# PART 3

Numerical Modeling and Results

# CHAPTER 3

Numerical Analysis and Comparative Results

## Chapitre 3

## Numerical Analysis and Comparative Results

#### 3.1 Introduction

In studying the effect of earthquakes on dams, most analyses have concentrated on horizontal motions of the structure and valley walls. Fewer works have considered hydrodynamic pressures due to vertical motions, or the role of surface waves at the free surface [7, 9]. This work examines the effects of surface gravity waves on the distribution of hydrodynamic pressures using finite element methods. Two cases are considered:

- 1. the p = 0 approximation at the free surface (classical assumption).
- 2. The linearized free-surface condition including surface waves.

Both incompressible and compressible fluids are treated. Numerical results for the Oued El Fodda gravity dam are presented, and comparisons are made in the time and frequency domains.

#### 3.2 Numerical model setup

The dam considered is Oued El Fodda, a 101 m high gravity structure with a vertical upstream face. A two-dimensional finite element reservoir model was constructed in MATLAB.

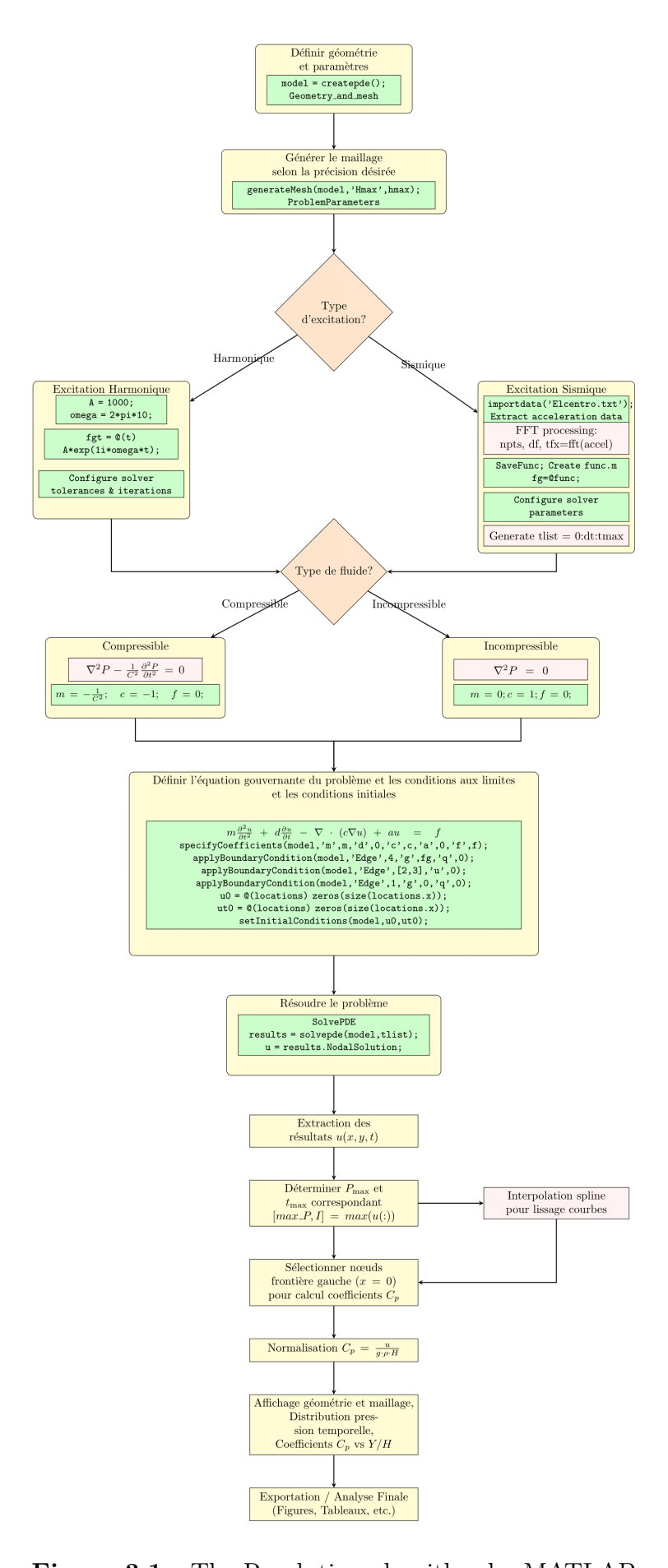
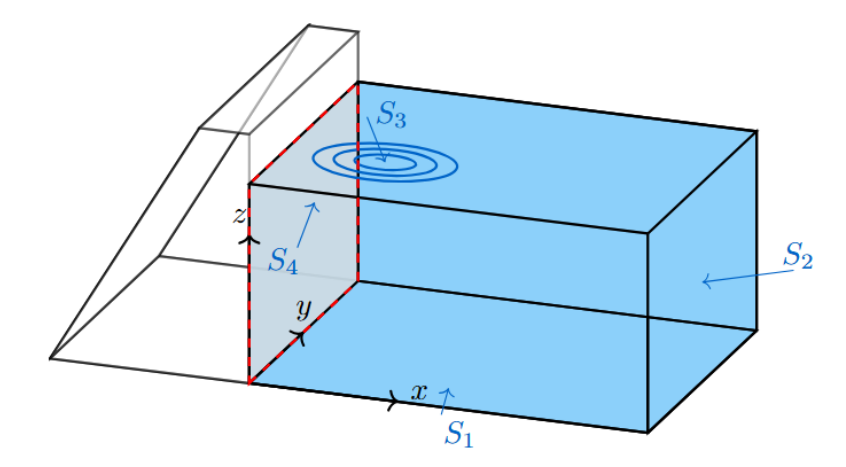


Figure 3.1 : The Resolution algorithm by MATLAB

- **Geometry**: The reservoir is represented with a height equal to (H = 100 m); upstream length taken sufficiently large to avoid reflections. See Section 3.3.1 for justification.
- **Mesh**: Triangular three-node elements; refinement near the dam-reservoir interface. Section 3.3.1 discusses mesh convergence in detail.
- Boundary conditions :
  - Upstream  $S_2$ : radiation condition  $(p(x, y, \omega) = 0)$ .
  - $\circ\,$  Dam–reservoir interface  $S_4$  : prescribed dam motion.
  - Reservoir bottom  $S_1$ : rigid bottom  $\frac{\partial p}{\partial y} = 0$ .
  - $\circ$  Free surface  $S_3$ :
    - 1. Without surface waves : p = 0,
    - 2. With surface waves :  $\frac{\partial p}{\partial y} + \frac{\omega^2}{g}p = 0$ .
- Excitations: Two types of loading are applied:
  - 1. Harmonic excitations over a range of frequencies,
  - 2. The 1940 El Centro earthquake record.

The dam—reservoir system with boundary conditions is shown in Fig. 3.2. The free surface, dam—reservoir interface, rigid bottom, and far-end truncation are indicated. This configuration is reduced in the following to a two-dimensional model.



**Figure 3.2 :** 3D schematic of the dam–reservoir system with boundary conditions and interface representation

#### 3.3 Baseline case: without surface waves

This case reproduces the classical assumptions of Westergaard, serving as a baseline for comparison. (p = 0 approximation).

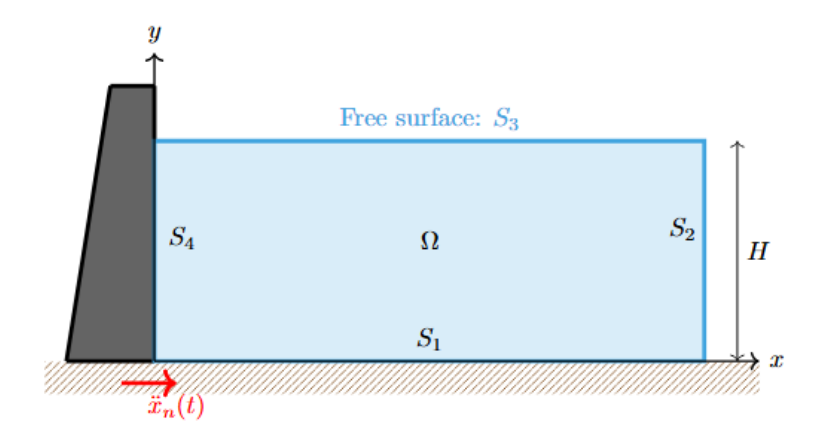


Figure 3.3: The dam–reservoir system

#### 3.3.1 Incompressible fluid-without surface waves

This section analyzes the hydrodynamic response of the dam—reservoir system using an incompressible fluid. First, the analysis establishes the appropriate reservoir length and mesh density. Then, it presents the resulting hydrodynamic pressure distributions.

#### 3.3.1.1 Determination of an appropriate reservoir length

The boundary condition on the reservoir's upstream side depends on the dam's height. Hydrodynamic pressure waves from structural vibrations propagate upstream without reflection and influence this boundary. It is assumed that far from the dam, where the distance is effectively infinite, the pressure becomes negligible. Typically, large dams have reservoirs extending far upstream from the structure. To investigate this, a parametric study was conducted to determine the optimal extent of the upstream region, defined by the reservoir length (L), as shown in Fig 3.4.

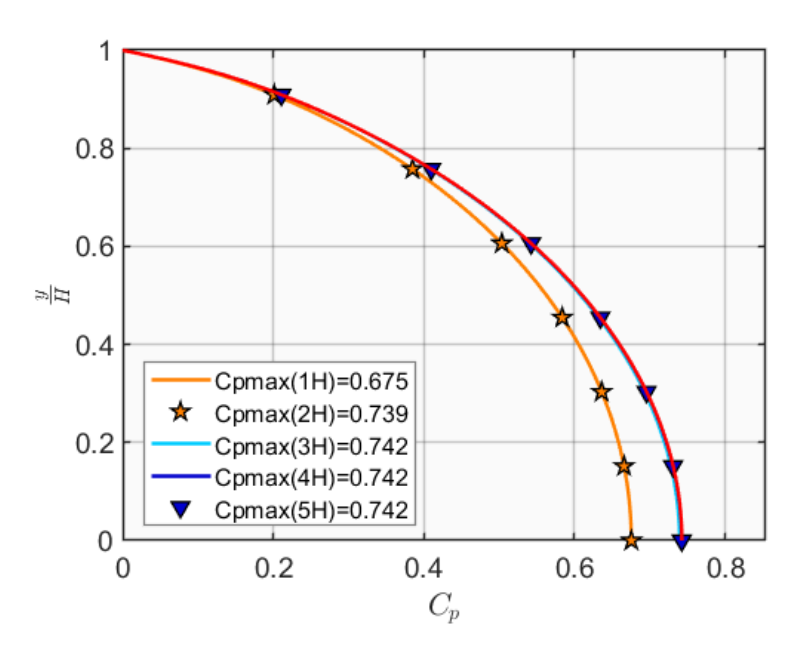


Figure 3.4: Comparison of hydrodynamic pressures for different lengths (L)

The results show that  $C_p^{max}$  converges for L=3H. Therefore, a reservoir length of 3H is adopted in the following analysis to ensure accuracy while minimizing computational cost (see Fig 3.5).

Length	Н	2H	3H	4H	5H
$C_{p_{\max}}$	0.675	0.739	0.742	0.742	0.742

**Table 3.1**: Convergence of  $C_{p_{\text{max}}}$  in a function of reservoir length.

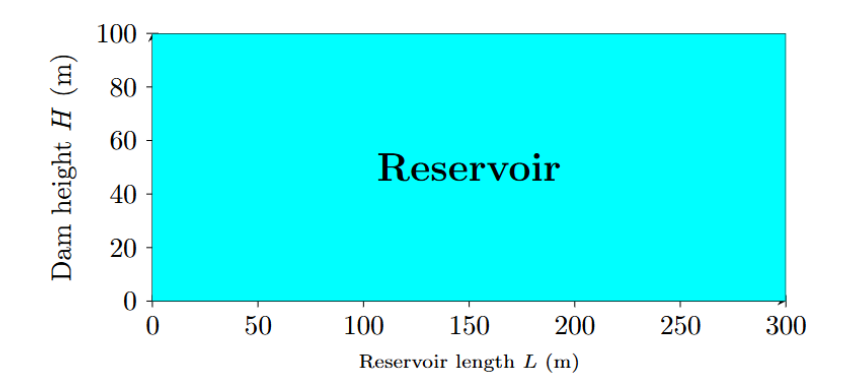


Figure 3.5 : Dam reservoir

#### 3.3.1.2 Determination of the optimal mesh

To ensure accuracy and efficiency, we determined the optimal mesh for the reservoir. A coarse mesh misses pressure gradients near the dam face, while an overly fine mesh raises computational costs without meaningful accuracy gains. We refined the mesh and tracked the maximum hydrodynamic pressure coefficient  $C_p^{max}$ . Mesh configurations are shown in Fig 3.6, and results are given in Table 3.2. Based on this study, a balance was achieved at the selected mesh, which provided accurate results for  $C_p^{max}$  with reasonable computational effort.

Number of nodes on the upstream face	Total number of nodes	Number of elements	$C_{p_{\max}}$
5	67	103	0.732
9	236	412	0.739
17	883	1648	0.741
33	3413	6592	0.742
65	13 417	26 368	0.742

**Table 3.2**: Influence of the number of mesh nodes on the upstream face of the dam on the hydrodynamic pressure coefficient  $C_p$ .

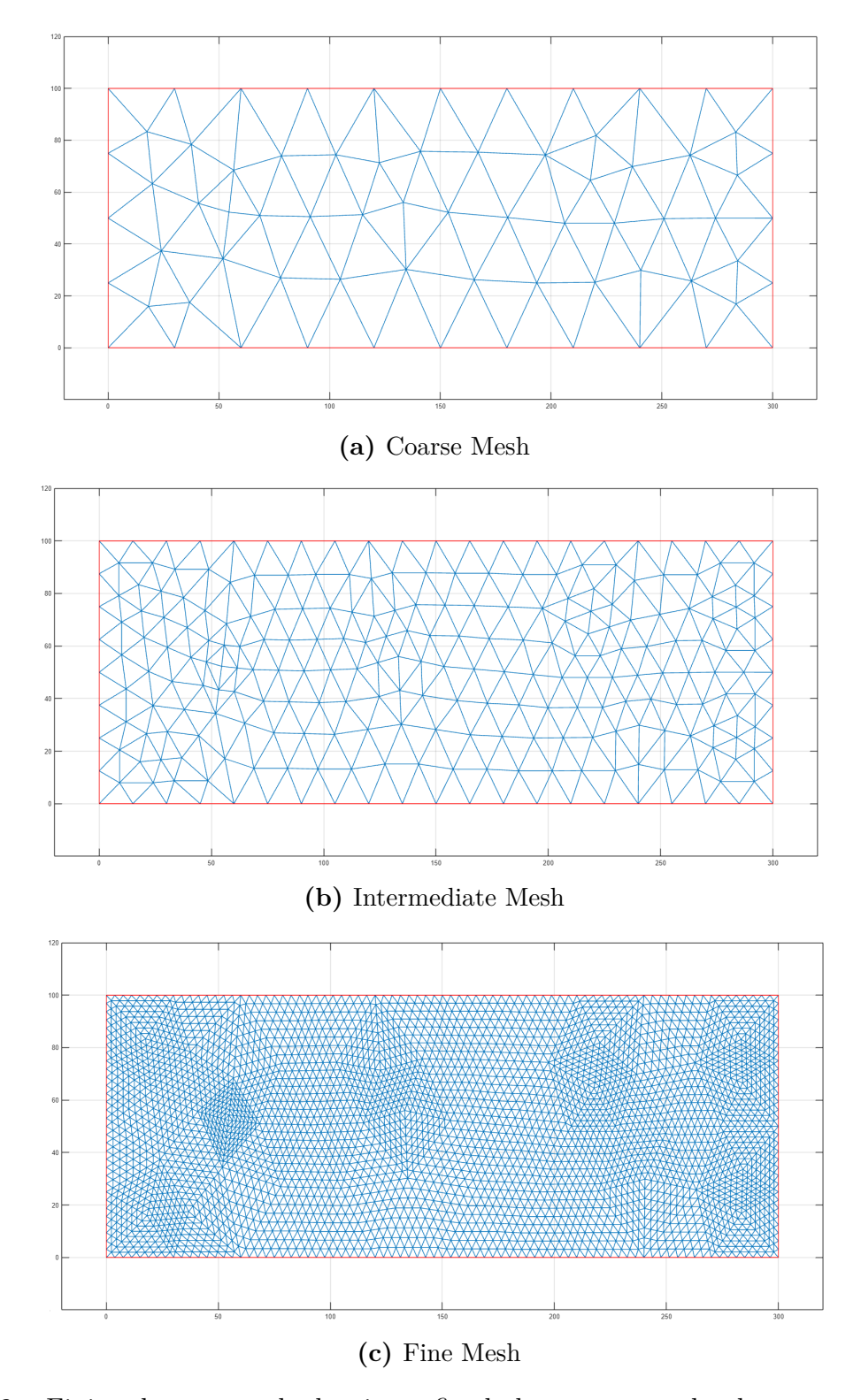


Figure 3.6 : Finite element mesh showing refined elements near the dam-reservoir interface (H = 100 m, L = 300 m).

#### 3.3.1.3 Results for an optimal mesh

Fig. 3.7 shows the isopressure contours from the finite element simulation. The color scale illustrates the spatial distribution of hydrodynamic pressures within the reservoir. Maximum values appear near the dam base, while pressures decrease progressively with elevation and approach zero at the free surface. The smoothly spaced contours reflect a stable pressure gradient, consistent with theoretical expectations.

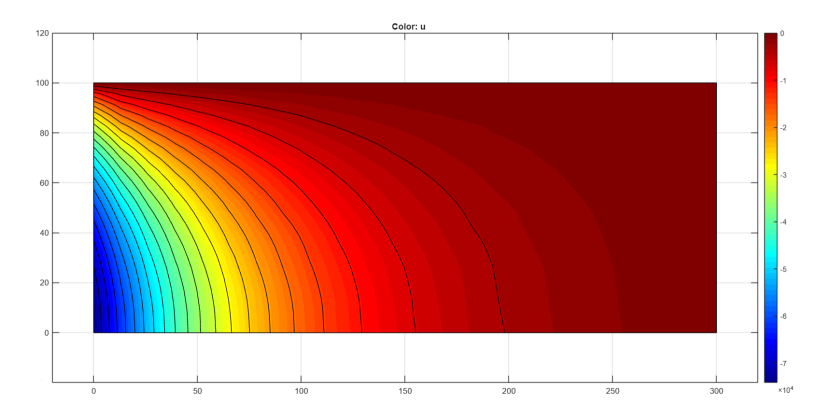


Figure 3.7: Contours of hydrodynamic isopressures

#### 3.3.2 Compressible fluid-without surface waves

The effect of water compressibility on hydrodynamic pressures was examined in the frequency domain.

#### 3.3.2.1 Case of a harmonic excitation

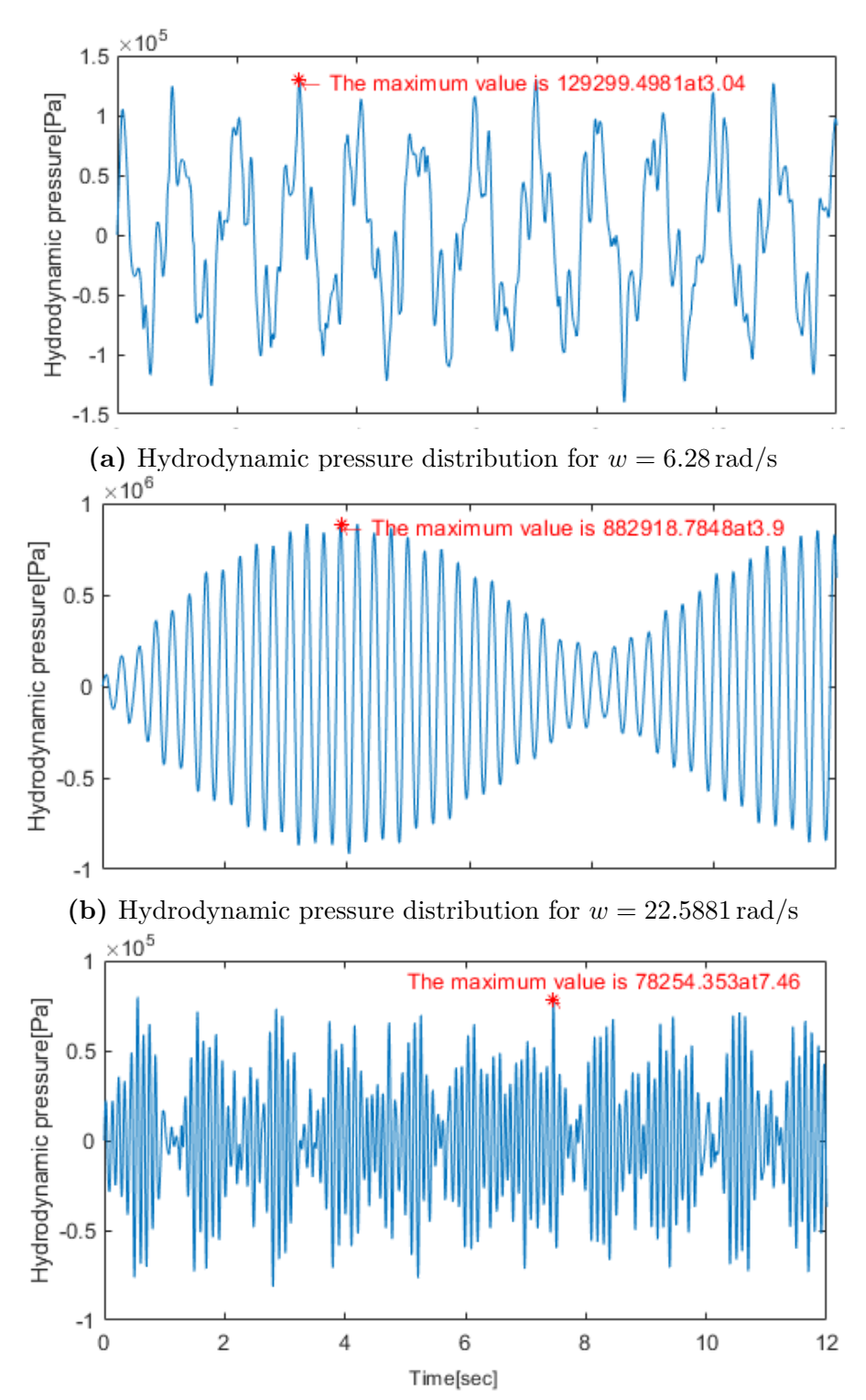
Pressures at the dam base were computed for f = 1, 3.6, 10 Hz Fig(3.8). Resonance occurred at f = 3.6 Hz, consistent with

$$f_{\text{resonance}} = \frac{C}{4H} = 3.6 \,\text{Hz}.\tag{3.1}$$

Maximum pressure reached  $8.7 \times 10^5 \,\mathrm{Pa}$  under resonance conditions

#### 3.3.2.2 Seismic excitation

For the El Centro earthquake input (Figs. 3.9–3.12), a significant time lag is observed between the excitation peak and the dam response. The seismic excitation reaches its maximum at t = 2.12 s, whereas the dam's hydrodynamic response peaks at t = 26.06 s, corresponding to a delay of 23.94 s. This phase shift reflects the influence of fluid compressibility, which slows the propagation of pressure waves in the reservoir and thus delays the dam's reaction to the seismic loading.



(c) Hydrodynamic pressure distribution for  $w = 62.8319 \,\mathrm{rad/s}$ 

**Figure 3.8**: Response to harmonic excitations  $f = 1, 3.6, 10 \,\mathrm{Hz}$ 

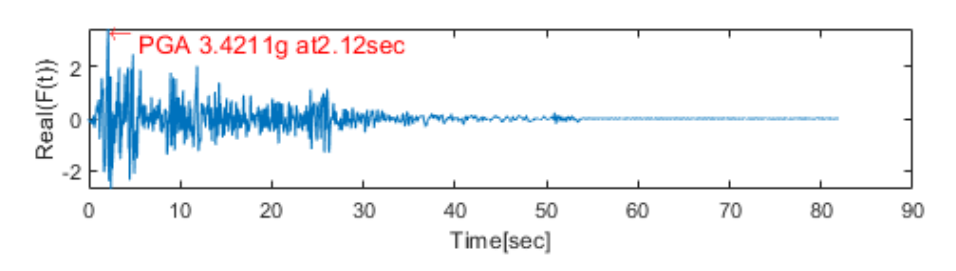


Figure 3.9: The seismic acceleration of El Centro, 1940

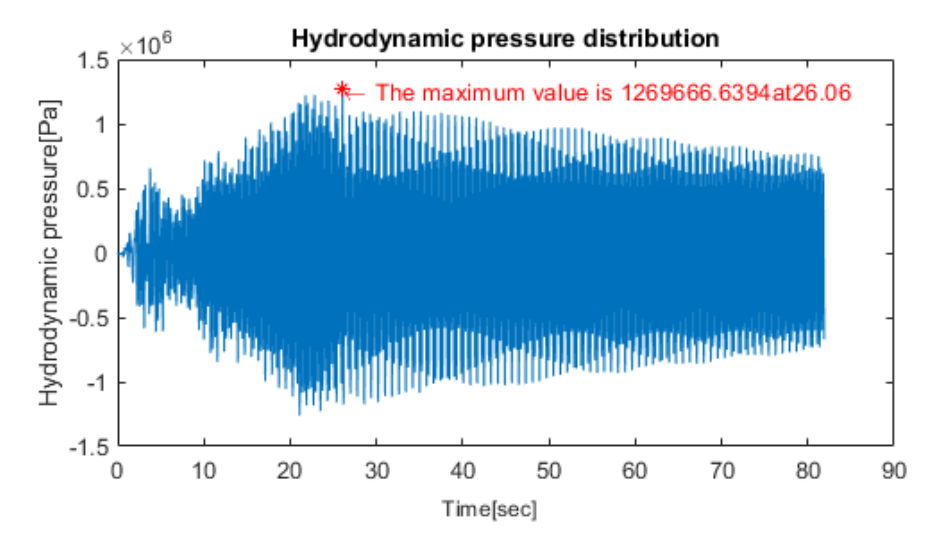


Figure 3.10: The response to a seismic excitation (EL CENTRO)

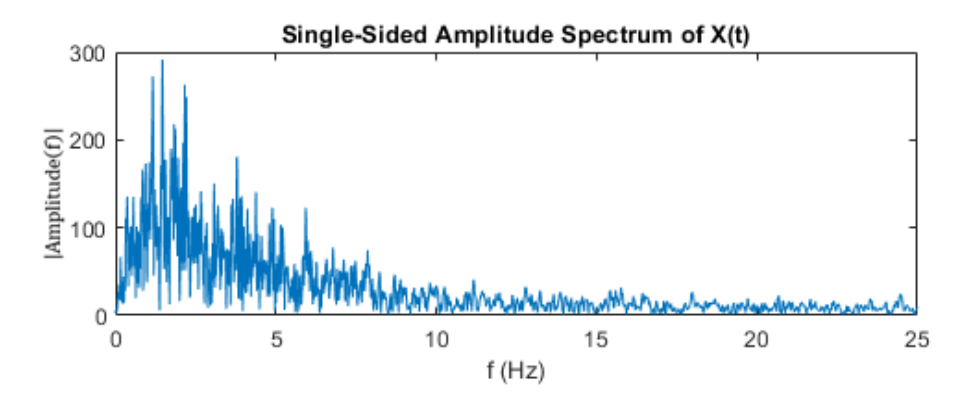
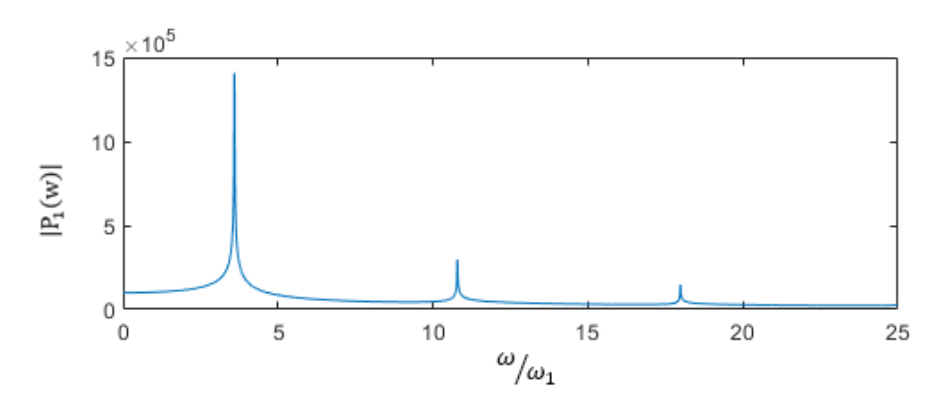


Figure 3.11: Fourier transform of the accelerogram



 ${f Figure~3.12:}$  Variation of hydrodynamic pressures as a function of excitation frequency at the base of a vertical rigid dam

#### 3.4 Extended case: with surface waves

Surface-wave effects were incorporated through the linearized free-surface boundary condition. Results were compared with the simplified approximation.

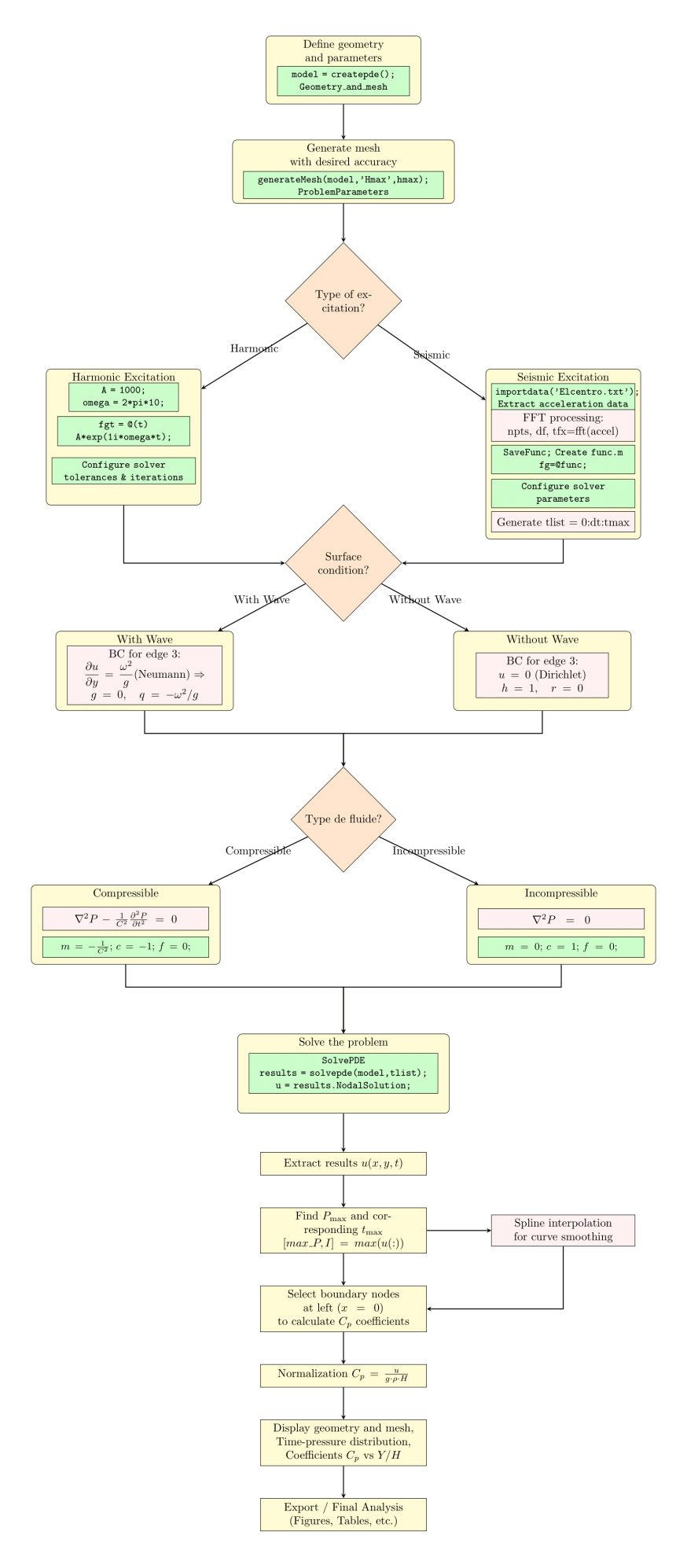


Figure 3.13: The resolution algorithm by MATLAB

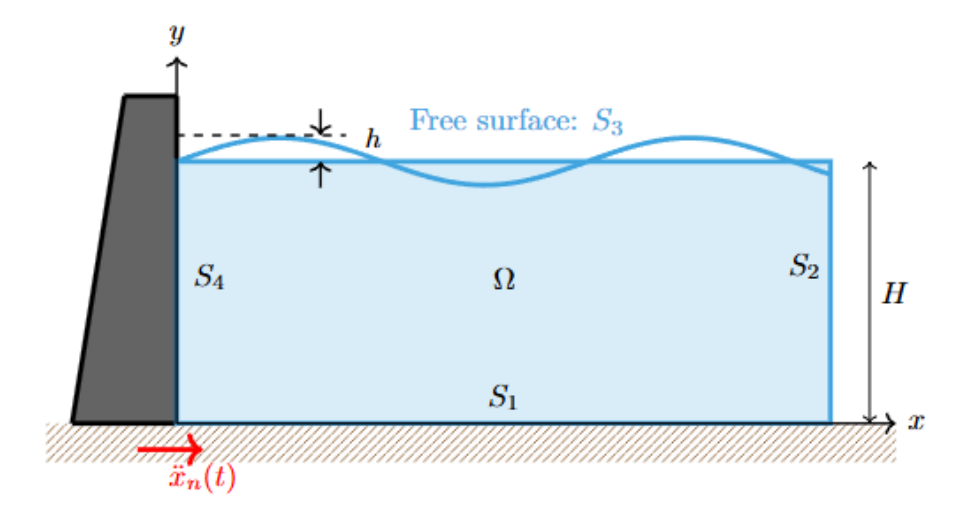


Figure 3.14: The dam-reservoir system with a surface wave above the fixed free surface

#### 3.4.1 Incompressible fluid—with surface waves

The investigation into the effect of surface waves on hydrodynamic pressure begins with the case of an incompressible fluid, a standard assumption in studies of gravitational surface waves [15, 16, 9, 6, 22]. This approach simplifies the analysis and allows the hydrodynamic response to be attributed solely to free-surface oscillations, providing a clear benchmark for comparison.

#### 3.4.1.1 The wave-effect parameter

The influence of free-surface oscillations was characterized by

$$\sigma = \frac{\omega^2 H}{g},\tag{3.2}$$

where  $\sigma$  is a dimensionless frequency parameter that characterizes the free-surface wave motion in the reservoir. It depends on the angular frequency  $\omega$ , the reservoir depth H, and the gravitational acceleration g. This parameter is related to the fundamental wave properties through the wavelength  $\lambda$ , the phase velocity C, and the wavenumber k, which are defined as:

$$C = \sqrt{\frac{g\lambda}{2\pi}}, \qquad k = \frac{\omega}{C} = \frac{2\pi}{\lambda}.$$
 (3.3)

These relations describe how the oscillation frequency and the depth of the reservoir determine the propagation of surface gravity waves. A larger value of  $\sigma$  corresponds to shorter wavelengths (higher frequencies), while smaller  $\sigma$  values indicate longer waves with slower propagation. Some works adopt the inverse form,  $Cw = 1/\sigma$ , but the physical interpretation remains equivalent.

Analytical benchmarks confirm that surface waves dominate for  $\sigma \lesssim 10$  and vanish for  $\sigma \gtrsim 200$  (Table 3.3).

$Fr^2 \ll 1$ (Slow Regime)			$Fr^2 \gg 1$ (Fast Regime)				
			Percentage				Percentage
$\sigma$	$C_p^{\max}$ (with wave)	$C_p^{\max}$ (with no wave)	deviation (%)	$\sigma$	$C_p^{\max}$ (with wave)	$C_p^{\max}$ (with no wave)	deviation (%)
0.1	0.007178	0.742613	99.03	1	0.113036	0.742616	84.77
0.2	0.015133	0.742616	97.96	2	0.245542	0.742616	66.93
0.5	0.044293	0.742616	94.03	3	0.403521	0.742616	45.66
0.6	0.055962	0.742616	92.46	4	0.500747	0.742616	32.56
0.7	0.068668	0.742616	90.75	5	0.560577	0.742616	24.51
0.8	0.082426	0.742616	88.90	20	0.742797	0.742616	-0.024
0.9	0.097228	0.742616	86.90	33	0.742797	0.742616	-0.024

**Table 3.3**: Comparison of maximum pressure coefficients with and without surface-wave effects in slow and fast regimes, obtained using the Triftz method.

#### 3.4.1.2 Analysis of hydrodynamic pressure contours

At low  $\sigma$ , negative pressures appeared near the surface and extended deep into the reservoir (Fig 3.15). With increasing  $\sigma$  ,negative regions contracted and pressures localized along the dam.

#### 3.4.1.3 Analysis of the velocity vector field

At small  $\sigma$ , coherent vectors radiated into the reservoir (Fig 3.16). For  $\sigma \geq 100$ , vectors diminished to a thin zone adjacent to the dam, an p = 0 approximation suffices.

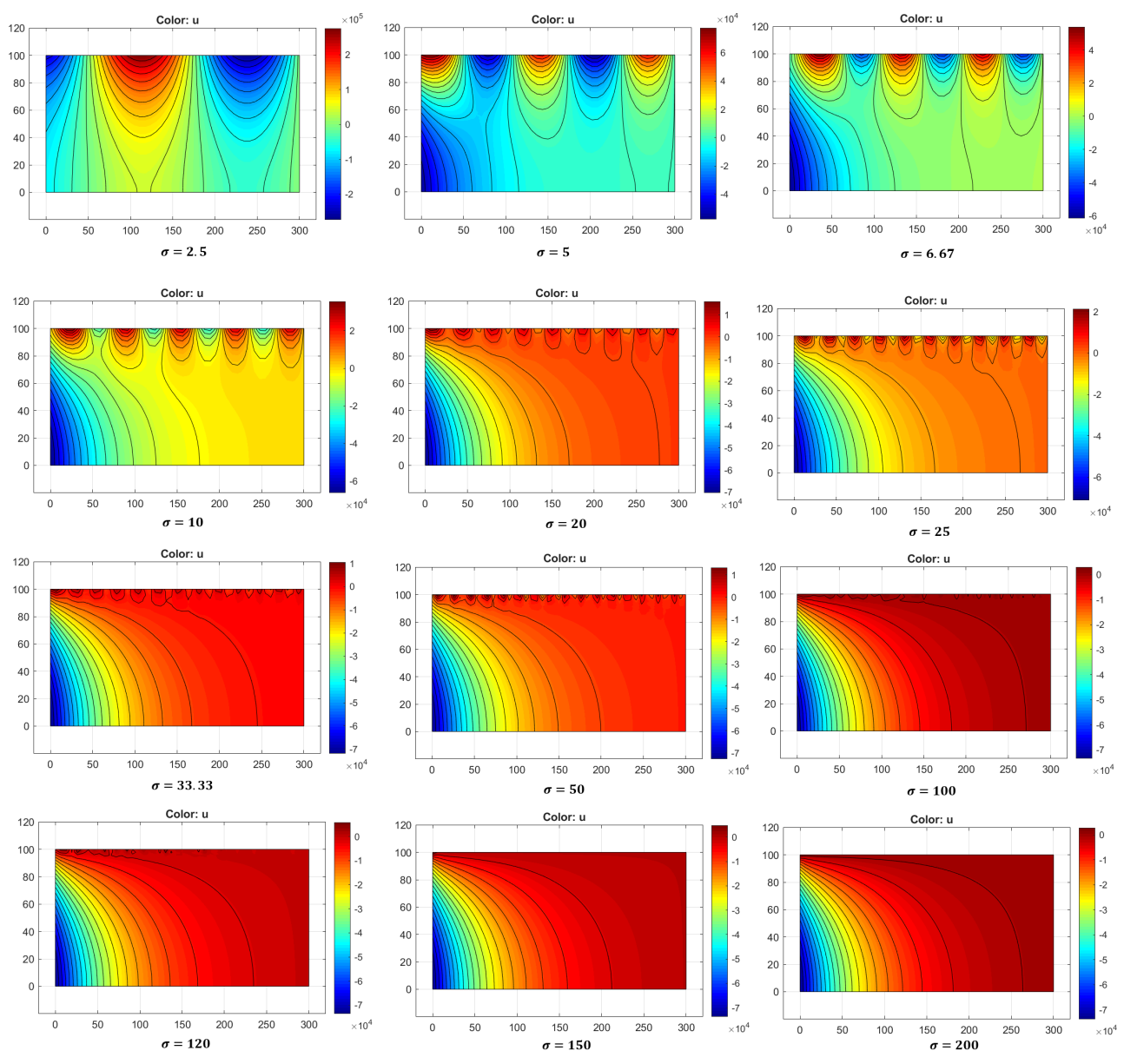


Figure 3.15 : Evolution of hydrodynamic pressure contours with the surface-wave parameter  $\sigma$ 

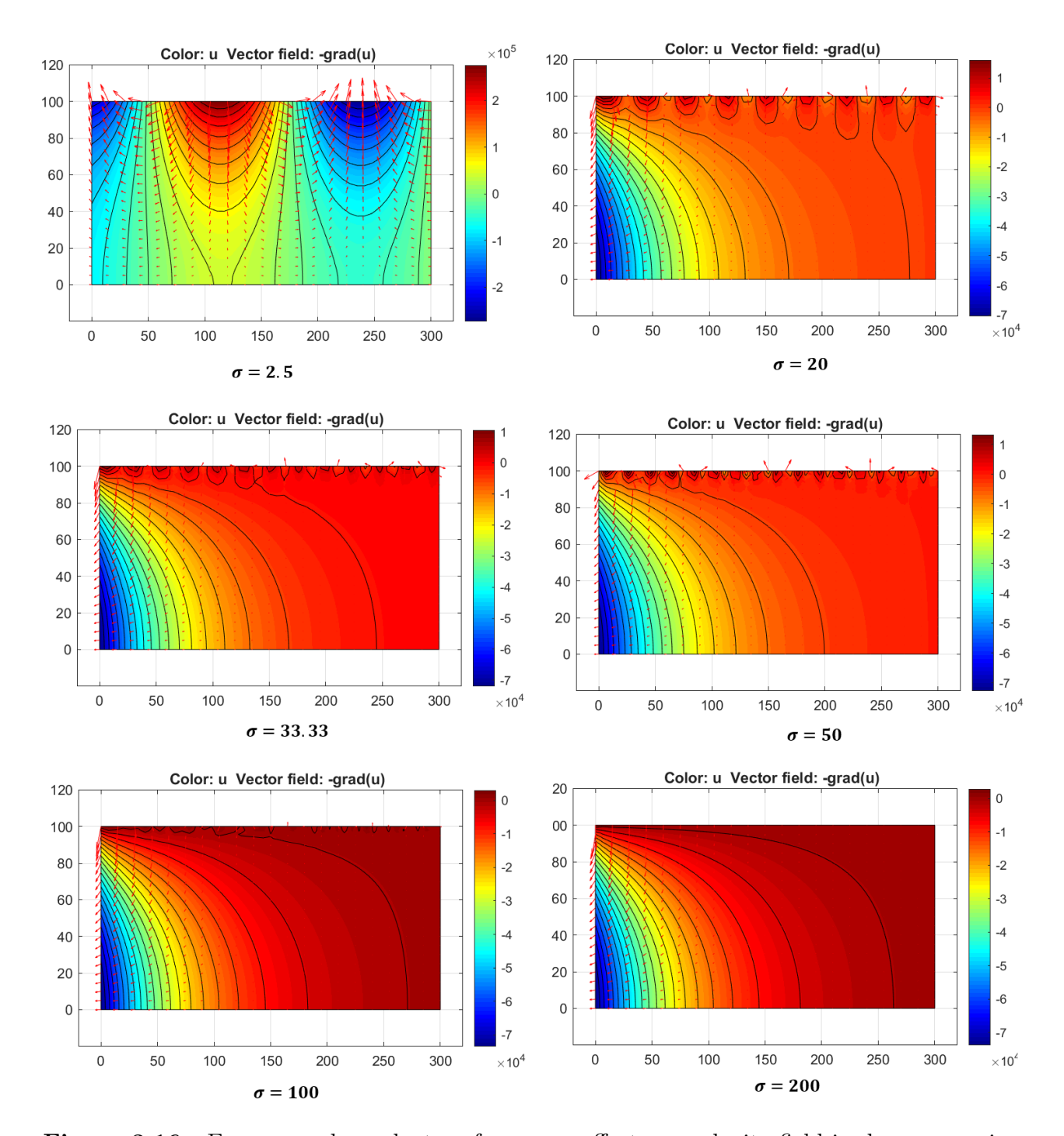


Figure 3.16: Frequency-dependent surface wave effects on velocity field in dam reservoir.

#### 3.4.1.4 Hydrodynamic pressure profiles for harmonic Excitation

Pressure distributions along the dam face were obtained for different values of the wave-effect parameter  $\sigma$  under harmonic excitation. (Figs. 3.17–3.18, Table 3.4)

**Table 3.4**: Maximum pressure coefficient  $C_p^{\text{max}}$  for a vertical dam under different values of the surface-wave parameter, assuming an incompressible, inviscid fluid.

$\sigma$	$C_p^{\max}$	$C_p^{\max}$	Percentage	
0	(no wave)	(with wave)	deviation (%)	
2.5	0.742	0.350	52.83	
3.33		0.467	37.06	
5		0.556	25.06	
30		0.717	3.36	
50		0.727	2.02	
80		0.733	1.21	
100		0.735	0.94	
200		0.739	0.40	
300		0.740	0.26	

#### 1. Effect of surface waves.

At low values of  $\sigma~(\approx 2.5)$  , the maximum pressure coefficient was reduced by more than 50% owing to surface-wave radiation. For intermediate values ( $\sigma=$  3–5) , the reduction ranged between 25–37%

#### 2. High-frequency limit.

For  $\sigma \geq 100$ , deviations became negligible (< 1%), and the solution approached the simplified assumption

#### 3. Profiles.

Pressures increased with depth and were maximum at the base. Near the surface, negative pressures appeared when surface waves were included

#### Observation

- Surface-wave effects dominate at low excitation frequencies ( $\sigma \leq 5$ ).
- For  $\sigma \geq 100$ , the simplified assumption p=0 at the free surface is sufficiently accurate.
- Negative pressures near the free surface are a characteristic feature of surface-wave radiation.

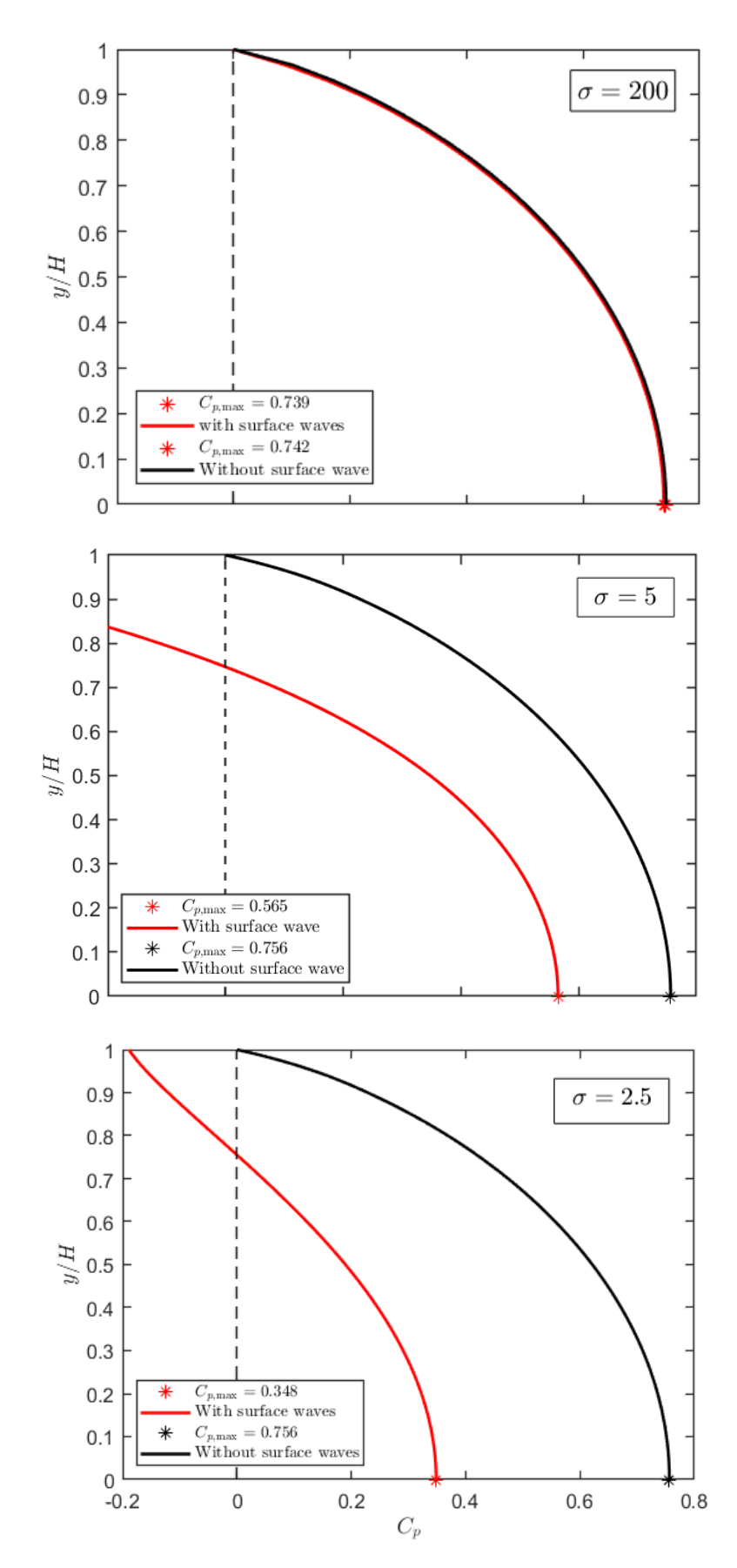


Figure 3.17: Variation of the pressure coefficient with depth for different values of the surface-wave parameter

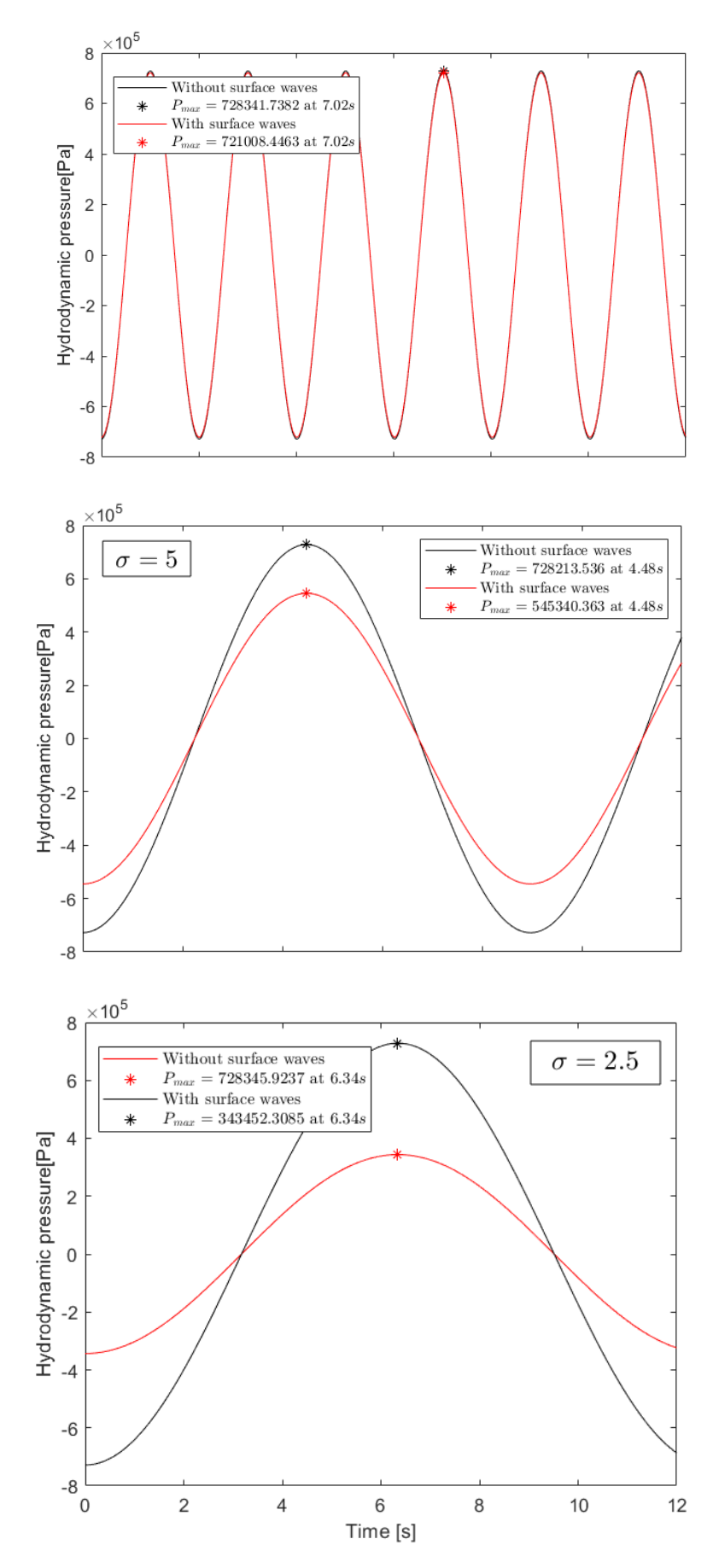


Figure 3.18: Hydrodynamic pressure response to surface waves for different values of the surface-wave parameter  $\sigma$  assuming an incompressible, inviscid fluid

#### 3.4.2 Compressible fluid—with surface waves

The compressibility of water modifies the hydrodynamic response, especially at high frequencies.

**3.4.2.0.1 Compressibility parameter.** The effect is characterized by the dimensionless parameter B [16], defined as

$$B = \frac{\omega H}{C},\tag{3.4}$$

where C is the speed of sound in water. Note that B can also be expressed in terms of the surface-wave parameter  $\sigma$  as :

$$B = \frac{\omega H}{C} = \frac{\sqrt{\sigma g H}}{H},\tag{3.5}$$

B represents the ratio of reservoir depth to acoustic wavelength. For  $B \ll 1$ , the fluid is nearly incompressible; for  $B \gtrsim 1$ , compressibility becomes important. For H = 100 m and C = 1438 m/s, values of B are given in Table 3.5.

$\sigma$	$\omega \text{ (rad/s)}$	B
2.5	0.495	0.034
5	0.700	0.049
100	3.130	0.218

**Table 3.5**: Computed values of the compressibility parameter B for different values of  $\sigma$ .

Since all values of B are well below unity, compressibility is of secondary importance in the present frequency range. At low  $\sigma$ , the response is governed by surface-wave radiation. At high  $\sigma$ , wave effects vanish and compressibility appears only as a phase lag in the pressure. The two effects do not peak simultaneously.

These observations are in line with the study of Tsai and Wei [17], who found compressibility to be important at high frequencies and surface waves to dominate at low frequencies, with negative pressures appearing near the free surface.

#### Seismic excitation

A seismic analysis was performed for both with and without surface wave effects using the El Centro 1940 record. Fig 3.19 shows the temporal distribution of hydrodynamic pressure at the reference point for the compressible case with surface-wave boundary condition. The peak hydrodynamic pressure at the reference point was

$$P_{\text{no-wave}} = 1.292 \times 10^6 \text{ Pa at } t = 26.06 \text{ s}, P_{\text{with-wave}} = 1.255 \times 10^6 \text{ Pa at } t = 22.82 \text{ s}.$$

The corresponding reduction was 2.87% (Table 3.6).

Case	Peak pressure (Pa)	Time of peak (s)
No waves	$1.292 \times 10^{6}$	26.06
With waves	$1.255 \times 10^{6}$	22.82

**Table 3.6**: Peak hydrodynamic pressures under El Centro excitation for both case with and without surface waves

For the El Centro earthquake (high-frequency input), the difference between the simplified assumption and the free-surface case was only 2.87%, indicating that surface-wave effects are negligible under seismic loading.

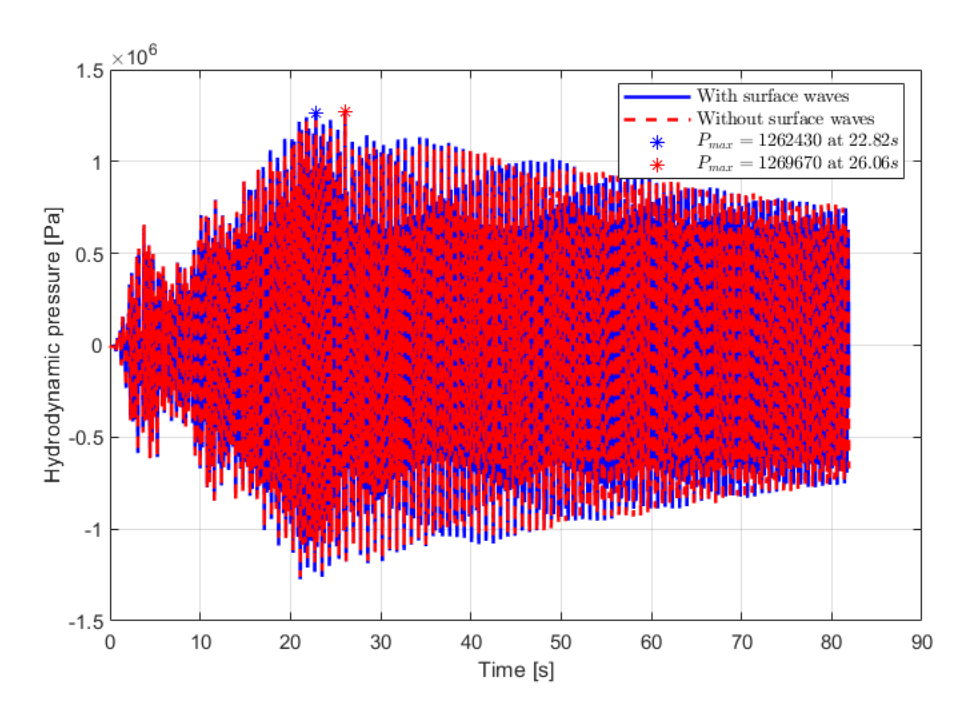


Figure 3.19 : Seismic response of hydrodynamic pressures including compressibility and surface-wave effects

#### 3.5 Comparison with classical studies

For completeness, the present numerical results were compared with the analytical criteria of earlier investigators. The comparisons show close agreement and help to clarify the conditions under which surface-wave and compressibility effects may be neglected.

#### 3.5.1 Nath (1969)

Nath introduced the relative frequency parameter

$$n = \frac{cT}{H},\tag{3.6}$$

For n = 30, he obtained

$$T = \frac{nH}{C} = \frac{30 \times 100}{1438} \approx 2 \text{ s},$$
 (3.7)

so that

$$\omega = \frac{2\pi}{T} \approx 3.141592654 \text{ rad/s}, \qquad \sigma = \frac{\omega^2 H}{g} \approx 100.6.$$
 (3.8)

At this frequency he reported that the pressure coefficient at the free surface was only 0.0002 with the linearized condition, compared to zero with p = 0. He concluded that surface waves would have some effect only when the relative frequency of motion is very small, and that for relatively high frequencies, where compressibility effects become significant, the assumption p = 0 at the free surface is sufficiently accurate.

The present FEM results show exactly the same behaviour. For low values of  $\sigma$  ( $\sigma \approx 2.5-5$ ) the pressures were reduced by more than 50% due to surface-wave radiation, but for  $\sigma \geq 100$  the difference from the the simplified assumption fell below 1%. Thus the numerical model confirms Nath's observation that surface waves vanish at high frequencies, while compressibility remains the controlling factor.

#### 3.5.2 Bustamante et al. (1963)

Bustamante and co-workers proposed limits for neglecting surface oscillations in terms of the ratio H/T. They showed that the error is less than 20% when

$$\frac{H}{T} > 2.6\sqrt{H},\tag{3.9}$$

and less than 5% when

$$\frac{H}{T} > 4.2\sqrt{H}.\tag{3.10}$$

For H = 100 m and  $\omega = 0.49$  rad/s,

$$T = \frac{2\pi}{\omega} \approx 12.82 \text{ s}, \qquad \frac{H}{T} = \frac{100}{12.82} \approx 7.8 \text{ m/s}.$$
 (3.11)

The thresholds are  $2.6\sqrt{H}=26.0$  m/s and  $4.2\sqrt{H}=42.0$  m/s, both far greater than the actual value. Accordingly, Bustamante's criterion predicts that surface waves are important in this regime. The FEM results confirm this prediction : at  $\sigma\approx 2.5$ , pressures were reduced by more than 50% relative to the rigid-lid assumption.

#### 3.5.3 Eatock Taylor (1981)

Eatock Taylor derived a simple inequality for neglecting surface waves:

$$\omega_1 > 8.3\sqrt{\frac{g}{H}}.\tag{3.12}$$

For H = 100 m this gives

$$\omega_{\text{lim}} = 8.3 \sqrt{\frac{9.81}{100}} \approx 2.60 \text{ rad/s.}$$
 (3.13)

From the present study, the resonance frequency was found to be  $\omega=22.5881$  rad/s Surfacewave effects were also shown to vanish for  $\sigma\gtrsim 100$ , which corresponds to  $\omega\approx 3.14$  rad/s. Since  $\omega=22.5881$  rad/s is far greater than both limits, the resonance lies firmly in the high-frequency regime. In this range, compressibility dominates, and surface-wave radiation can be neglected. The FEM confirms this: at resonance, the deviation between the with and without surface waves cases was less than 1%, while at low excitation frequencies ( $\sigma\lesssim 5$ ) reductions exceeded 50%. The conclusion is therefore the same as that of Eatock Taylor, namely that the assumption p=0 is accurate for high frequencies, but surface waves must be retained at low ones.

#### 3.6 Conclusion

The finite element formulation reproduced classical results when surface waves were neglected, confirming the validity of the simplified assumption p=0 at the free surface. When surface waves were included, significant reductions in hydrodynamic pressures were observed at low excitation frequencies ( $\sigma \leq 5$ ), reaching more than 50%. At higher frequencies ( $\sigma \geq 100$ ) the deviations became negligible, and the simplified condition was found to be sufficient. The presence of surface waves also introduced negative pressures near the free surface, a feature absent in the classical case. Fluid compressibility played only a secondary role in the frequency range considered, producing a slight phase lag but little change in amplitude. Under harmonic excitation close to resonance, hydrodynamic pressures reached values of the order of  $10^6$  Pa, while for seismic input (El Centro 1940 record), the effect of surface-wave radiation was limited to a small reduction ( $\approx 2.9\%$ ) in peak pressures. Overall, the results demonstrate that surface-wave effects must be included at low frequencies, but that fluid inertia remains the dominant factor in realistic seismic loading.

# GENERAL CONCLUSION

### General Conclusion

The hydrodynamic response of a rigid vertical dam subjected to both harmonic and seismic excitations has been examined using the finite element method, considering both compressible and incompressible fluids, as well as surface-wave effects. The free-surface condition was introduced in both the frequency and time domains to evaluate its significance on the pressure distribution.

For harmonic excitation, surface waves proved to be decisive at low frequencies. Negative pressures developed at the reservoir surface, accompanied by a marked reduction of pressures at the base. For the case of the vertical El Fodda dam, the base pressures were reduced by nearly 50% when surface waves were included, showing that their omission can lead to severe overestimation. At higher frequencies, surface-wave effects became negligible, and compressibility governed the response.

For seismic excitation, compressibility introduced a significant phase delay between the ground motion and the hydrodynamic response. In the El Centro record, the acceleration reached its maximum at 2.12 seconds, whereas the peak pressure was attained at 26.06 seconds, a delay of nearly 24 seconds. The inclusion of surface waves in this case altered the maximum pressure by only 2.9%, indicating that their contribution under earthquake loading is minor compared with that of compressibility.

It is concluded that surface waves have a strong influence on the hydrodynamic response in low-frequency harmonic excitation, whereas compressibility is the dominant effect under seismic input. Simplified models neglecting these phenomena may lead to misleading estimates of hydrodynamic pressures and should be applied with caution.

#### Perspectives

The present formulation is limited to a two-dimensional rigid dam-reservoir system with a linearized free-surface condition. Several extensions are possible :

- The inclusion of dam flexibility and soil-structure-fluid interaction would allow a more realistic representation of coupled dynamics.
- A three-dimensional reservoir model would capture wave propagation and diffraction effects not present in the 2D case.
- Nonlinear free-surface motion should be considered under strong seismic excitation, where wave steepening and breaking may occur.
- The role of reservoir bottom absorption, sediments, and variable bathymetry requires further investigation.

Chapitre 3 General Conclusion

- The inclusion of viscosity and turbulence may refine the prediction of energy dissipation in real reservoirs.

# Bibliographie

### Bibliographie

- [1] Abdelmadjid Tadjadit. Investigations analytique et numérique des effets de compressibilité et de viscosité sur le comportement sismique des barrages rigides à géométrie irrégulière. PhD thesis, Ecole Nationale Polytechnique, El Harrach, Alger, Algérie, 2018. Thèse de Doctorat.
- [2] Maity D and Bhattacharyya S.K. A parametric study on fluid–structure interaction problems. *Journal of Sound and Vibration*, 263(4):917–935, 2003.
- [3] Maity D and Bhattacharyya S.K. Time-domain analysis of infinite reservoir by finite element method using a novel far-boundary condition. *Finite Elements in Analysis and Design*, 32(2):85–96, 1999.
- [4] Papazafeiropoulos G, Tsompanakis Y, and Psarropoulos P.N. Dynamic interaction of concrete dam-reservoir-foundation: Analytical and numerical solutions. In M Papadrakakis, N. D. Lagaros, and M. Fragiadakis, editors, *Proceedings of COMPDYN-2009: 2nd International Conference on Computational Methods in Structural Dynamics and Earth-quake Engineering*, pages 22–24, Rhodes, Greece, 2009.
- [5] Eatock Taylor R. A review of hydrodynamic load analysis for submerged structures excited by earthquakes. *Engineering Structures*, 3(3):131–138, 1981.
- [6] Attarnejad R and Zahedi H. Effect of surface waves on dam-reservoir interaction during the earthquake. In *Proceedings of the International Conference on Computational & Experimental Engineering & Science*, pages 1–6, Madeira, Portugal, 2004.
- [7] Avilés J and Suárez M. Effects of surface waves on hydrodynamic pressures on rigid dams with arbitrary upstream face. *International Journal for Numerical Methods in Fluids*, 62:1155–1168, 2010.
- [8] Calvi A. Analytical interpretation of hydrodynamic pressure on dams. Technical report, Technical Report, 2024.
- [9] Wu Y.C. and Yu D.J. Trefftz method for hydrodynamic pressure on rigid dams with non-vertical upstream face. *International Journal for Numerical Methods in Fluids*, 9:1–7, 1989.
- [10] Bustamante J.I., Rosenblueth E., Herrera I., and Flores A. Presión hidrodinámica en presas y depósitos [hydrodynamic pressure in dams and reservoirs]. *Boletín de la Sociedad Mexicana de Ingeniería Sísmica*, 1(2):37–54, 1963.
- [11] Gogoi I and Maity D. A novel procedure for determination of hydrodynamic pressure along upstream face of dams due to earthquakes. In *Proceedings of the 14th World Conference on Earthquake Engineering*, Beijing, China, 2008.

Chapitre Bibliographie

[12] Kotsubo S. Dynamic water pressure on dams during earthquakes. In *Proceedings of the* 2nd World Conference on Earthquake Engineering, pages 799–814, 1960.

- [13] Anil K. Chopra. Hydrodynamic pressures on dams during earthquakes. *University of California, Berkeley, Structural Engineering Laboratory*, Report No. 66-2:1–50, 1966.
- [14] Nath B. Hydrodynamic pressures on high dams due to vertical earthquake motions. *Proceedings of the Institution of Civil Engineers*, 44:7171–7189, 1969.
- [15] Chwang A.T. Effect of stratification on hydrodynamic pressures on dams. *Journal of Engineering Mathematics*, 15(1):49–63, 1981.
- [16] Huang L.-C. and Chwang A.T. Seismic water pressures on dams for arbitrarily shaped reservoirs. Technical Report IHR Report No. 291, Iowa Institute of Hydraulic Research, The University of Iowa, 1985.
- [17] Ching-Piao Tsai and Tzu-Kun Wei. Hydrodynamic pressure on an oscillating vertical plate. In *Mechanics Computing in 1990's and Beyond*, pages 399–403. ASCE, 1991.
- [18] Martin P.A. Havelock wavemakers, westergaard dams and the rayleigh hypothesis. *Journal of Engineering Mathematics*, 26:267–280, 1992.
- [19] Pani P.K. and Bhattacharyya S.K. Hydrodynamic pressure on a vertical gate considering fluid-structure interaction. *Finite Elements in Analysis and Design*, 44(12):759–766, 2008.
- [20] Chen B.-F. and Yuan Y.-S. Hydrodynamic pressures on arch dam during earthquakes. Journal of Hydraulic Engineering, 137(1):34–44, 2011.
- [21] Abdollahi M and Attarnejad R. Dynamic analysis of dam-reservoir-foundation interaction using finite difference technique. *Journal of Central South University*, 19(5):1399–1410, 2012.
- [22] Da Silva S.F. and Pedroso L.J. Interaction dam-reservoir: study of conservative and dissipative effects. Revista Ibracon de Estruturas e Materiais, 12(4):858–873, 2019.
- [23] International Commission on Large Dams (ICOLD). Selecting Seismic Parameters for Large Dams. Bulletin 148 (Revision of Bulletin 72). ICOLD, Paris, France, 2016.
- [24] Seghir A. Investigation des effets d'interaction sismique fluide-structure par couplage éléments finis éléments infinis [investigation of seismic fluid-structure interaction effects using finite-infinite element coupling]. Master's thesis, École Nationale Polytechnique, Alger, Algérie, 1999.
- [25] Santosh Kumar Das, Kalyan Kumar Mandal, and Arup Guha Niyogi. Finite element-based direct coupling approach for dynamic analysis of dam-reservoir system. *Innovative Infrastructure Solutions*, 8:44:1–15, 2022.
- [26] Gogoi I and Maity D. Influence of sediment layers on dynamic behavior of aged concrete dams. *Journal of Engineering Mechanics*, 133(4):400–413, 2007.
- [27] Nath B. Hydrodynamic pressures on arch dams during earthquakes. *Proceedings of the Institution of Civil Engineers*, 25:165–175, 1963.
- [28] Islam Haouas and Amir Saker. Application de la méthode des éléments finis dans les calculs dynamique et hydrodynamique des structures. *Mémoire de Projet de Fin d'Études*, 2023. Étude dynamique d'une paroi moulée sous sollicitation sismique avec Plaxis 2D.

Chapitre Bibliographie

[29] Abdelmadjid Tadjadit. Pressions hydrodynamiques sur barrages rigides à fruits irréguliers sous excitations sismiques. Master's Thesis, École Nationale Polytechnique, Algiers, 2010.

## Appendices

# Annexe – Extension of the Previous Work to Inclined Rigid Dams Using Analytical Formulations

**Note:** The results presented in this appendix represent preliminary findings from ongoing research conducted in collaboration with my supervisor and provide additional analytical context that complements the main thesis results. A complete analytical extension will be published separately.

#### .1 Introduction

This annex presents selected results that originate from a scientific article prepared jointly with my supervisor, currently under review in *LARHYSS JOURNAL*. These results are included solely as supplemental material to allow comparison between the analytical formulations developed in external research and the numerical results presented in the main body of this dissertation. The content here does not constitute the entirety of the article; rather, it serves to illustrate the consistency and limits of the numerical and analytical approaches as a natural extension of this end-of-study project.

#### .2 Formulation

The governing wave equation was expressed in terms of a velocity potential and expanded in Trefftz functions. Boundary conditions were imposed at the reservoir bottom, the free surface (with and without gravity-wave terms), the radiation boundary, and along the dam face inclined at an angle  $\theta$  to the vertical. Two fluid models were considered: (a) incompressible, inviscid; (b) compressible, viscous, the latter represented by the Kelvin–Voigt model. The dispersion relation arising from the free-surface condition was solved iteratively by the Newton–Raphson method. Solutions yield hydrodynamic pressure distributions and resultant forces on the dam face.

Chapitre Bibliographie

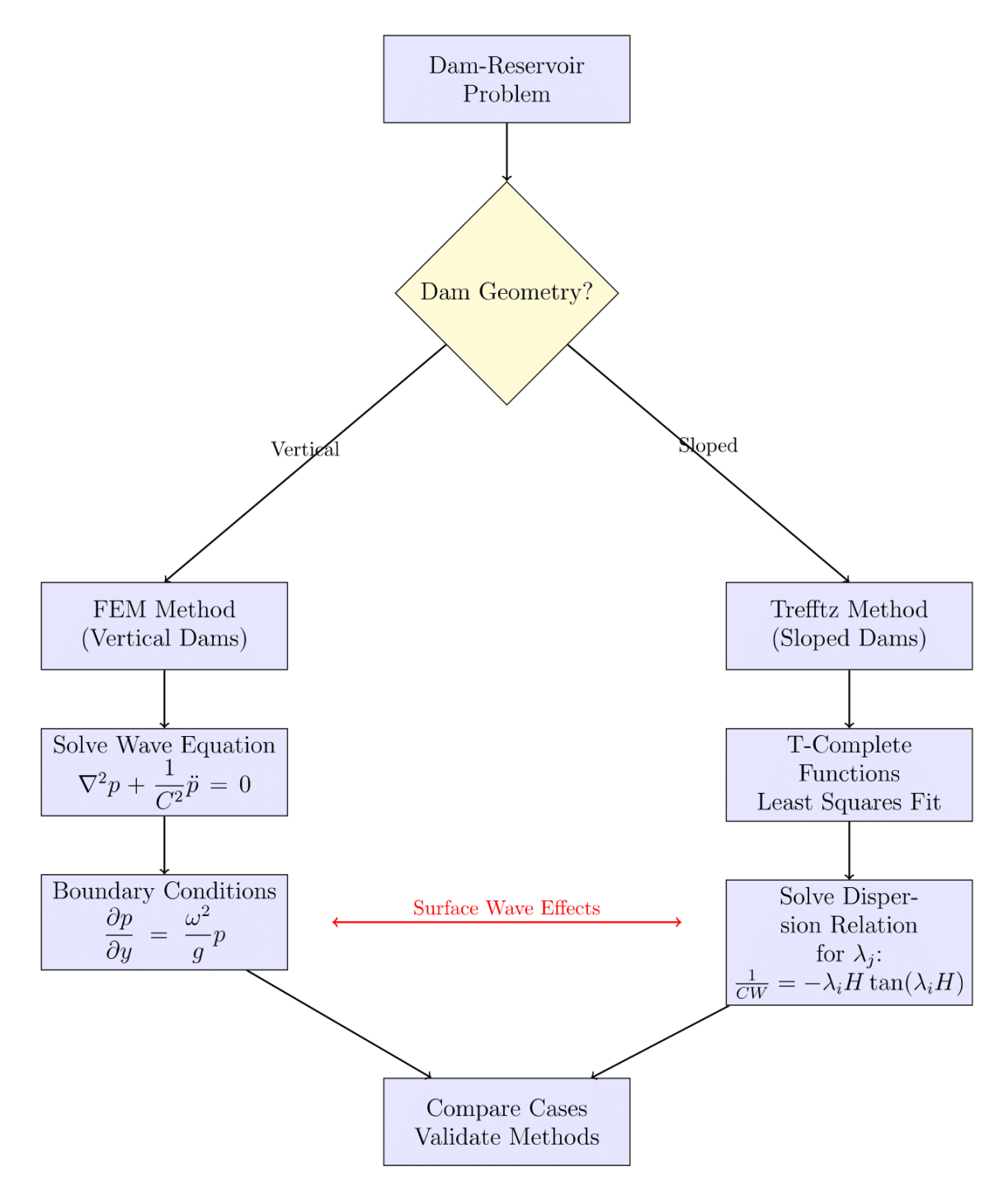


Figure 20: Methodological framework comparing FEM approach (vertical dams) and Trefftz method (sloped dams).

#### .3 Results

The following principal observations were made:

- 1. For vertical dams ( $\theta = 0^{\circ}$ ), surface waves reduced hydrodynamic pressures markedly at low excitation frequencies, by more than 50%. For inclined dams, the reduction persisted but was smaller: about 38% at 15° and 24% at 30°.
- 2. Negative pressures were observed near the free surface whenever gravity-wave terms were included.

Chapitre 3 Bibliographie

3. Increasing dam inclination consistently lowered pressure coefficients, in comparison with the vertical case.

- 4. For compressible, viscous fluids, resonance peaks in shear force and overturning moment were strongly damped. In this regime, viscosity dominated the response.
- 5. while the effect of surface waves was negligible. The analytical extension also highlights the combined influence of surface gravity waves and dam inclination, which significantly modifies the hydrodynamic pressure distribution near the free surface.

#### .4 Discussion

It is seen that the effect of surface oscillations is essentially confined to low frequencies. Inclination of the upstream face, and viscosity of the reservoir fluid, both act to diminish hydrodynamic demands on the dam. These results extend the finite-element findings of the main thesis, which showed that surface-wave effects become negligible under seismic input.

#### .5 Conclusions

The principal conclusions are:

- Surface waves affect pressures only at low frequencies; their influence is negligible under seismic loading.
- Inclination of the dam face reduces pressures substantially relative to the vertical case.
- Viscosity introduces damping at resonance, moderating dynamic responses.

Thus, while both finite element and Trefftz formulations confirm the limited role of surface waves at seismic frequencies, the latter further demonstrates the beneficial effects of slope and damping. The two approaches together yield a consistent and complementary picture of damreservoir interaction.